Open access • Journal Article • DOI:10.1029/RG009I003P00773

Large-scale properties of the interplanetary magnetic field — Source link

Kenneth H. Schatten

Institutions: Goddard Space Flight Center

Published on: 01 Aug 1971 - Reviews of Geophysics (John Wiley & Sons, Ltd)

Topics: Interplanetary magnetic field, Dipole model of the Earth's magnetic field, Heliospheric current sheet, Solar wind and Mercury's magnetic field

2 (mix)

X-692-71-96
PREPRINT

NASA TM X-65467

LARGE SCALE PROPERTIES OF THE INTERPLANETARY MAGNETIC FIELD

KENNETH H. SCHATTEN

MARCH 1971

GSFC — GODDARD SPACE FLIGHT CENTER —
GREENBELT, MARYLAND

PRESENTED AT THE CONFERENCE ON THE SOLAR WIND AT ASILOMAR, CALIFORNIA

X-692-71-96

LARGE-SCALE PROPERTIES OF THE INTERPLANETARY MAGNETIC FIELD

Kenneth H. Schatten
Laboratory for Extraterrestrial Physics
NASA-Goddard Space Flight Center
Greenbelt, Maryland 20771

March 1971

TABLE OF CONTENTS

Abstract

Our knowledge of the large-scale properties of the interplanetary magnetic field is reviewed. The early theoretical work of Parker is presented along with the observational evidence supporting his Archimedes spiral model. The discovery of interplanetary magnetic sectors is reviewed. The variations present in the interplanetary magnetic field from the spiral angle are related to structures in the solar wind. The causes of these structures are found to be either non-uniform radial solar wind flow or the time evolution of the photospheric field. The relationship of the solar magnetic field to the interplanetary magnetic field is also reviewed. The direct extension of solar field-magnetic nozzle controversy is discussed along with the coronal magnetic models and their relation to the interplanetary magnetic field. The effect of active regions upon the interplanetary magnetic field is discussed with particular reference to the evolution of interplanetary sectors. The variation of the interplanetary magnetic field magnitude is shown throughout the solar cycle. The percentage of time the field magnitude is greater than 10 gammas closely parallels sunspot number. The suggested influence of the sun's polar field on the interplanetary field and alternative views of the magnetic field structure out of the ecliptic plane are presented. In addition, a variety of possible interplanetary field structures are discussed.

I. Introduction

Our knowledge of the large-scale properties of the interplanetary magnetic field began with Parker's work in 1958. Parker reasoned that the kinetic energy of the solar wind plasma as it left the sun should decrease as r^{-2} whereas the magnetic energy density would decrease as r^{-4}. It followed, therefore, that the general solar dipole field would not significantly influence the motion of the outflowing gas once the gas left the solar corona. Parker then considered the "frozen-in" magnetic field configuration of interplanetary space. By "frozen-in" field lines, it is generally meant field lines which obey the equation $\vec{E} + \vec{v}/c \times B = 0$ or in terms of a simple physical picture, the field lines are constrained to move with the plasma flow. The field lines thus follow the stream lines of the plasma, which, for a rotating sun and radially flowing solar wind, is the Archimedean spiral configuration. Figure 1 from Parker (1958) shows such an Archimedean spiral field for a solar wind flowing at 1000 km/sec. Parker (1963) later revised the solar wind speed to 300 km/sec to correspond to quiet periods; this resulted in the near 45° average interplanetary magnetic field direction from the sun-earth line. Whether or not the solar active region fields contributed to the general streaming of gas from the sun as proposed by Biermann (1951) was an open question. The magnetic energy density associated with the active region fields was very much larger than that associated with the background solar field. Much more energy would be required to extend these fields into interplanetary space; thus only the background solar field was thought to extend into interplanetary space.

Other than Parker's theoretical treatment of the interplanetary magnetic field, our knowledge of its properties has developed mostly on theories and observations based directly on the results of space experiments. A variety of magnetometers have been employed in the study of the interplanetary magnetic field, the most common of which is the fluxgate magnetometer. The measurement of the interplanetary magnetic field is difficult due to the low field strength. The field is typically 5 gammas where 1 gamma equals 10^{-5} gauss. An extensive review of the use of various magnetometers for space research has recently been completed by Ness (1970a).

Some early evidence showing agreement with Parker's interplanetary field model was presented by Davis (1964) at the last solar wind conference in 1964. Figure 2 shows a scatterplot of the observed interplanetary magnetic field from Mariner 2. ΔB_z corresponds to field pointed away from the sun and ΔB_y to field in the direction opposite to the spacecraft motion about the sun. Each point represents a "smoothed"hourly average of 5 successive hourly averages. The dashed line shows the expected result for the Parker spiral field model. As Davis noted, despite the averaging, one must surely be "impressed by the disorder and irregularity in these measurements". This point was dramatically illustrated in the movie of the interplanetary magnetic field by Wilcox et al. (1966), where a great deal of variability was seen on a short time scale. This variability, of course, relates to structural properties of the field.

In addition to the unexplained structural variations, our knowledge of the origin of the interplanetary magnetic field was also rather limited at the last solar wind conference. Since this time much knowledge

has been acquired concerning both the structural variability and the origin of the interplanetary magnetic field. It is the purpose of this paper to outline much of this work and to discuss gaps in our understanding concerning some of these points.

Large-Scale Spatial Structure

A. Quasi-Stationary Structure

The early work of Ness and Wilcox (1964) showed that the interplanetary magnetic field had a 27-day periodicity and that it correlated with the average direction of the photospheric magnetic field during three successive solar rotations near the minimum of the last sunspot cycle. The 27-day periodicity was related to the 27-day rotation period of the sun as seen from the earth. This supports Parker's hypothesis that the sun was the origin of the interplanetary magnetic field. A 4-1/2 day time lag was found for their highest correlations, representing the time necessary for a radially flowing solar wind to transport the solar magnetic field to a position near the earth.

It was found that the interplanetary magnetic field as observed near the earth had a tendency to point predominantly "away-from-the-sun" or "toward-the-sun" (along Parker's theoretical spiral angle) for a duration of several days. This repeated every 27 days and formed a pattern which was given the name sector structure. This early sector structure pattern is shown in Figure 3 from Wilcox and Ness (1965). The plus signs indicate away-from-the-sun magnetic field and the minus signs, toward-the-sun field. As can be seen, a definite pattern emerges. There were four sectors, three approximately equal in size and one, half as large as the other three. In a reference frame rotating with the sun this pattern was quasi-stationary in time and persisted possibly for longer than a year (Fairfield and Ness, 1967).

B. Interplanetary Magnetic Field Mapping

In order to better understand the large-scale structure of the interplanetary magnetic field, a means of mapping it was sought. One approach to mapping the field is shown in Figure 4 from McCracken and Ness (1966). The 7.5minute average magnetic field was projected into the ecliptic plane and the vectors were placed end to end. The scale of this figure is such that it extends a distance of 5×10^6 km or about 0.03 AU. Localized "kinks" or "regressions" were observed in the magnetic field. The "kinks" in the magnetic field are significant in that high energy particles are affected by them as they travel through space. Figure 4 shows, in addition to the magnetic field structure, the cosmic ray anisotropy on December 30, 1965. During this period, the solar-generated cosmic radiation, arriving at the earth, was markedly anisotropic and varied in direction considerably. As Figure 4 shows, despite major changes in the interplanetary magnetic field direction, the cosmic ray anisotropy remained well aligned with the field. Thus the cosmic ray anisotropy can be thought of as a measurement of the average field direction over the scale of gyroradius of the particles. The observations by McCracken and Ness of occasional abrupt changes in cosmic ray anisotropy suggested to them that the interplanetary magnetic field was filamentary in nature. This model of interplanetary field filaments has some times been referred to as the "spaghetti" model. Its geometry shown in panel H of Figure 30.

Although the method of mapping the interplanetary magnetic field employed by McCracken and Ness works well on a small scale in considering

the large-scale field structure, it is necessary to consider the effects of solar rotation and field transport due to the solar wind flow

At first glance, a time sequence of local magnetic measurements from a single spacecraft at 1 AU would seem inadequate to determine the large-scale geometry of the interplanetary magnetic field. This, however, is not necessarily the case, if the feature under investigation exhibits certain properties that allow extrapolations of the structure of the field. These basic properties are the rapid convection of the field away from the sun, the high conductivity of the solar wind plasma which inhibits the field from diffusing a substantial distance, the relatively constant nature of the source of the field, and the relatively steady direction and slowly varying magnitude of the solar wind velocity. These last two conditions are at times invalid, resulting in magnetic field extrapolations which are not meaningful. It is usually evident from the field patterns which incorrectly show a nonzero field divergence that one of the conditions has been violated.

Utilizing a steady radial solar wind velocity, one obtains the following relationships concerning the behavior of the interplanetary magnetic field with distance from the sun:

$$B_r (R_1) = B_r (R_o) (R_o/R_1)^2 \qquad (1)$$

$$B_\phi (R_1) = B_\phi (R_o) (R_o/R_1) \qquad (2)$$

$$B_\perp (R_1) = B_\perp (R_o) (R_o/R_1) \qquad (3)$$

B_r, B_ϕ, and $B_\perp$ are the three solar ecliptic components of the magnetic field. R_0 and R_1 are two radial distances from the sun. An extrapolation of the field is then made, taking into account corotation of the field and the radially flowing plasma. Figure 5 from Schatten et al.(1968) shows this extrapolated magnetic field in the plane of the ecliptic for December 1963, prepared from the IMP-1 magnetic field measurements of Ness et al. (1964). The gaps in the circle at 1 AU represent times when the IMP-1 satellite was near perigee (and therefore within the region influenced by the geomagnetic field) and interplanetary field observations could not be obtained. The data progress clockwise in time since the sun rotates counterclockwise, as seen from the north ecliptic pole. The solid curved line at the bottom separates observations taken 27 days apart. This is the time period necessary for a position on the sun facing earth to return to the same location. A 400 km/sec solar wind speed and a synodic period near 27 days was employed in this and all the figures of its kind. In addition, a circle with a dot in it, a circle with a cross in it, or an eight sided star are employed to indicate strong northward or strong southward oriented field or fine scale field fluctuations, respectively.

As can be seen, the magnetic field calculated is generally well represented by an Archimedean spiral. The sector boundary on day 336 is well-defined. Some of the field lines are more radially oriented and others more curved than the average Archimedes spiral. The main point, though, is that the field lines have the same topology as the Archimedean spiral geometry. The field lines can be "tied" to the

sun and directed into interplanetary space past the orbit of the earth. The whole system may corotate with little change for many solar rotations.

C. Magnetic "Kinks" and Velocity Gradient Variations.

The field lines in Figure 5 are occasionally distorted from a uniform spiral configuration; it is important to understand how such "distorted" structures arise. Schatten (1968) analyzed, to first order, the effect of radial (or temporal), azimuthal, and poloidal solar wind velocity gradients upon the magnetic field structure. The structures analyzed were the large scale kinks, similar to those shown in Figure 5 on days 343 and 352.

If one considers the magnetic field embedded within an element of plasma flowing radially away from the sun with an assumed azimuthal velocity gradient, one obtains the following equations governing the components of the field variation with radial distance:

$$B_r(R_1) = B_r\ (R_o)\ (R_o/R_1)^2 + B_\phi(R_o)\ (R_o/R_1)^2(1-R_1/R_o)1/v\ \frac{dv}{d\phi} \qquad (4)$$

$$B_\phi(R_1) = B_\phi\ (R_o)\quad (R_o/R_1) \qquad (5)$$

$$B_\perp(R_1) = B_\perp\ (R_o)\quad (R_o/R_1) \qquad (6)$$

Computations in the table discussed next are based upon values of R_o chosen to correspond to a position close to the sun where the velocity gradient has not caused substantial changes in the magnetic field pattern, and a value of R_1 at 1 AU where the field is observed. Table I shows that if one assumes azimuthal velocity gradients were responsible for the change in field direction, the directions computed

using the ratio of equations 4 and 5 above and the solar wind velocity measurements of the MIT plasma probe (next to last column) agree quite well with the observed field directions (last column). The interplanetary magnetic field spiral angle computed from the average (for each time period in Table I) solar wind velocity is in considerable disagreement for these time periods. This indicates that there were regions near the sun at this time emanating plasma at different velocities rather than a single source for each sector with a smooth temporal velocity variation.

Let us now consider in a more general way the causes of these substantial alterations of the magnetic field from the Archimedean spiral geometry. Close to the sun the plasma is partially constrained by the strong magnetic field to rotate with the sun. Beyond a few solar radii the plasma velocity becomes more radial than azimuthal. At these distances the corotation speed is substantially less than the solar wind velocity. The magnetic field has on the average an almost radial direction with a small, but important, azimuthal component which depends on the rotation rate of the sun. Beyond this distance the magnetic field is altered continually by the flow of the solar wind according to the equation:

$$\vec{dB}/dt = (\vec{V} \cdot \nabla)\ \vec{B} + \frac{\partial \vec{B}}{\partial t} = -\vec{B}(\nabla \cdot \vec{V}) + (\vec{B} \cdot \nabla)\vec{V} \qquad (7)$$

Thus the initial field after a five day transit from sun to earth may be computed from the following equation:

$$\vec{B}(R_1) = \int_0^T (-\vec{B}(\nabla \cdot \vec{V}) + (\vec{B} \cdot \nabla)\vec{V})\ dt \qquad (8)$$

where T equals 5 days and R_1 is 1 AU. Under steady-state conditions,

with a constant radial solar wind velocity this condition implies a spiral magnetic field. The first term in the integrand of equation 8 can serve to increase or decrease the field magnitude but not alter its direction. The last term is responsible for the changing direction of the magnetic field. The only manner in which the magnetic field can "know" at what angle to point is by gaining knowledge of the rotation rate of the sun. The velocity field, being radial, carries no such information. Thus the small, initial azimuthal magnetic field serves to inform the interplanetary field of this rotation. The information is transmitted and amplified by the solar wind through the dyadic term involving the velocity. Any addition gradients in the velocity field as a result of temporal or spatial variations in the solar wind velocity would tend to significantly alter the interplanetary field direction from the Archimedean spiral angle due to the integration and differentiation of the solar wind velocity in Equation 8. This is exemplified by the previous structures, where modest longitudinal velocity gradients resulted in significant alterations in the field geometry. This may become more important at greater radial distances from the sun as will be seen in Section II-F.

D. Dynamic Effects Upon Field Structure

The dynamic effects of flares will be treated briefly in Section III-E and more thoroughly by Hundhausen (1971). What is considered in this section are the dynamic effects of a variable source field near the sun. In addition to the possibility of solar wind velocity variations casuing a non-Archimedean spiral interplanetary

magnetic field, a variable source of magnetic field near the sun may also produce a non-spiral field geometry. In this case, the magnetic field near the sun no longer is oriented radially with a slight azimuthal component but rather has some other field geometry which is then frozen into the plasma and transported to 1 AU. If no large scale velocity perturbations exist to disrupt the pattern it may then be observed.

Figure 6 shows the interplanetary magnetic field in the ecliptic plane for November 1-9, 1965 from Schatten et al. (1968). A new feature is suggested in these observations in this figure. Magnetic loops are observed that consist of field lines that appear to leave the sun, reach into interplanetary space, and then connect back to the sun. This magnetic loop configuration represents a dynamic process, in so far as these field lines cannot remain in this shape in a quasi-stationary configuration. This configuration is convected out by the solar wind to form new spiral field lines. The looped field pattern is an enlargement of a structure that presumably existed in the corona five days before it was observed at 1 AU. It is thus necessary to examine the relationship between the interplanetary magnetic field and source of the field near the sun. This particular feature is discussed in greater detail in Section III-F.

E. Magnetic field Diffusion

Coleman and Rosenberg (1970) using Mariner 2, 4 and 5 data, have observed an effect in the interplanetary magnetic field, the physical cause of which is not quite clear. It may, however, relate to magnetic field diffusion in interplanetary space. They have investigated, in

detail, the north-south component of the interplanetary magnetic field. They observe a skewing of the magnetic field away from the solar equatorial plane. A particularly good example of their result is shown in Figure 7 using the Mariner 4 observations. Twenty-seven day running average values of B_θ are computed for toward and away sectors separately. Each average is shown by a dot for toward-the-sun field or a plus sign for away-from-the-sun field. The averages are computed every 3 days. The other quantities calculated are indicated on the figure. As is shown in Figure 7, Mariner 4 was below the solar equatorial plane from day 347 of 1964 until day 230 of 1965. As can be seen $B_{\theta s}$, which represents the field skewing, follows closely with heliographic latitude. The solid curve represents a fit proportional to solar latitude. This effect is equivalent to a skewing of the magnetic field away from the solar equatorial plane.

If the field were "frozen-into" the solar wind, the velocity would follow the same pattern. They estimate this would require a 30 km/sec north-south directed solar wind velocity component. The magnitude of V_θ for the same overlapping 27-day averages, using the MIT group's plasma velocities, was typically one third that required for the alignment of $\vec{B}$ and $\vec{V}$*. Furthermore, the sign of the velocity was opposite to that required for alignment, in that the observations indicated the solar wind velocity was directed towards the plane of the solar equator and the magnetic field directed away. The meaning of their observations is not quite clear, however, magnetic reconnection or in other words, field

*Rosenberg in a private communication has recently informed me that his calculations of b_{θ_+}, related to solar wind velocity, are uncertain for this time period.

diffusion is a possibility that might account for these observations. This suggestion is very tentative; as yet there is no physical explanation for their observations.

F. Radial Variation of the Interplanetary Magnetic Field.

In this section, we shall consider what is actually known about the radial variation of the interplanetary magnetic field. Figure 8 from Burlaga and Ness (1968) shows the interplanetary magnetic field variation from 0.8 to 1.0 AU as observed by Pioneer 6 in 1966. The figure shows the transverse and radial components of the field as well as the magnitude as a function of radial distance. The dashed line corresponds to Parker's theoretical model. Burlaga and Ness observe that the measurements are consistent with Parker's model. Coleman and Rosenberg (1968) analyzed the radial variation of the interplanetary magnetic field between 0.7 and 1.0 AU with similar results.

Coleman et al. (1969) utilized the observations of Mariner 4 to ascertain the radial dependence of the field from 1.0 to 1.5 AU. Figure 9 from Coleman et al. shows the joint distribution of pairs of components at a radial distance of 1.5 AU and colatitude 95.2°. The distribution of field components appears to be rather similar to the distribution at 1.0 AU. Figure 10 shows the mean values they obtain for various field component magnitudes as a function of radial distance. The quantities B, B_L, B_p and $|B_r|$ compare well with the theoretical values from Parker's model. Coleman et al. also calculated the variation of many quantities according to the best fit to a function of the form $C_o r^k$. Of interest are the exponents of the radial, azimuthal, and

north-south components of the magnetic field. In accordance with a "frozen-in" field and a uniform radial velocity flow these values should be -2., -1., and -1., respectively. Coleman et al. calculate values of -1.46, -1.27, and -1.29 with RMS deviations near 0.02. Thus the exponent values for the three field components are nearly equal and thus are decreasing in a more isotropic fashion than would be expected for Parker's model. As was suggested by the equations in Section II-C, the dyadic term $\nabla \vec{V}$ can serve to alter the configuration of the magnetic field in the solar wind. If the velocity variations become sufficiently large, the magnetic field direction is altered according to equation (8) and the field does not point along the appropriate Archimedean spiral angle. This results in a randomizing effect upon the field direction and thus a more isotropic behavior than would be suggested by Parker's model.

This aspect of magnetic field behavior is apparent in the calculations of Coleman et al. concerning the field direction, They fit the tangent of the spiral angle with a function of the form $C_o r^k$ and obtain a value of k equal to 0.16 rather than 1.0. Thus, although the solar wind appears capable of orienting the interplanetary magnetic field in accordance with the spiral model out to 1 AU; beyond this point it becomes increasingly ineffective.

It is necessary to mention that in these analyses of the variation of the interplanetary magnetic field with radial distance, temporal variations due to changing solar activity could cause effects which would apparently be related to radial distance. Coleman et al. attempted to remove this aspect of the problem by analyzing a data

set with a low geomagnetic activity index, thus removing temporal variations by insuring a somewhat uniform amount of solar activity. The results were nearly equal to those obtained with the entire data set, thus suggesting that the interplanetary field variations observed were indeed mainly due to radial influences.

It thus appears that the magnetic field components obey the Parker spiral model quite well from 0.7 to 1.0 AU. The magnitude of the field also decreases in accordance with the Parker spiral model from 1.0 to 1.5 AU. The directional aspects of Parker's spiral model appear not to be obeyed as well by the interplanetary magnetic field out to 1.5 AU. The field appears to show a large amount of isotropic behavior Processes occur which alter the direction of the magnetic field as it is convected outwards, and the random nature (and increasing strength as a function of radial distance) of these processes may be responsible for the disagreements between the observations of Coleman et. al. and Parker's idealized model. These processes may be waves, shocks, or high speed streams. Panel H in Figure 30 showing "chaotic" fields may describe the behavior of the interplanetary magnetic field at a few AU.

III. Relationship to Solar Features

A. Early Thoughts Concerning the Source of the Interplanetary Magnetic Fields

Parker's (1958, 1963) analysis appears to imply that the source of the interplanetary field is the general solar field. For mathematical simplicity, Parker assumed the solar field to be a dipole. Ahluwahlia and Dessler (1962) suggested that the polarity of the interplanetary magnetic field might be related to the observations of the photospheric magnetic field. Inspection of solar magnetograms taken by Babcock and Babcock (1955) suggested to Ahluwahlia and Dessler that the spiral field be divided into tubes of flux whose diameters range in size from .1 AU to 1 AU at the orbit of the earth. Each tube would contain only field lines of a single sense (toward- or away-from-the-sun).

B. Direct Extension of Solar Fields-Solar Magnetic Nozzle Controversy

First evidence for the interplanetary magnetic field being of solar origin was obtained by Ness and Wilcox (1964). They showed that the direction of the interplanetary magnetic field had a 27-day periodicity and that it correlated well with the average direction of the photospheric magnetic field during three solar rotations near the minimum of the last sunspot cycle. Although high correlations were found for many latitudes, the recurrence period of the interplanetary magnetic field suggested a source on the photosphere 10° to 15° from the equator. The large-scale "sector" property of the interplanetary magnetic field which was previously discussed in section II was also noted.

The large scale sector ordering of the interplanetary magnetic field has led Davis (1965) to suggest that the interplanetary sectors originated

from small regions on the sun, essentially "nozzles", in which the field was essentially undirectional. A contrary opinion has been supported by Wilcox (1968) where a "mapping" hypothesis allows the sector to originate from large, well-ordered magnetic structures on the sun in which there is a tendency for each longitude near the sun to be connected to a longitude at the orbit of the earth by magnetic field lines.

The amount of "nozzling" or non-radial flow is an important concern. The maximum one might expect would occur if all the field lines from a sector originated in a single sunspot. This would be about a 1:3000 area expansion above that which would occur from direct radial flow. Thus the source of the unidirected sectors was debated. Did they arise from a small-scale, large magnitude, unidirected field on the sun or a large scale, weak field? The "source surface" model, now to be discussed, sheds some light on this question.

C. "Source Surface" and "Zero-Potential" Magnetic Models

Magnetic models have been developed by Altschuler and Newkirk (1969) and Schatten et al.(1969) that allow calculations of the coronal magnetic field from the observed photospheric magnetic field. Figure 11 from Schatten et al. (1969) is a schematic representation of these two similar models. The topology of the magnetic field in the solar corona as suggested by the magnetic models may be examined in Figure 11. There are three distinct regions in these models where different physical phenomena occur. Region 1 represents the photosphere, where the magnetic field motion is governed by the detailed motions of the plasma near the photosphere. Above the photosphere the plasma density diminishes very rapidly with only moderate decreases in the magnetic energy density.

This results in region 2, where the magnetic energy density is greater than the plasma energy density and hence controls the configuration. One may then utilize the force-free condition, $\vec{j} \times \vec{B} = 0$, and in fact make the more restrictive assumption that region 2 is current free. The magnetic field in Region 2 may then be derived from a potential that obeys the Laplace equation: $\nabla^2 \phi = 0$. The scalar potential may then be employed in this region. Substantially further out in the corona the total magnetic energy density diminishes to a value less than the plasma energy density, and the magnetic field can no longer structure the solar wind flow. The magnetic field has, however, become oriented very much in the radial direction, as suggested by Davis (1965). Thus, before the total magnetic energy density falls below the plasma energy density, a region is reached where the transverse magnetic energy density does so. It is the transverse magnetic field that interacts with the coronal plasma, since a radial magnetic field would neither affect nor be affected by a radially flowing plasma. Regions 2 and 3 are separated by the surface where the transverse magnetic energy density falls below the plasma energy density. In region 3 transverse magnetic fields are transported away from the sun by the radially flowing plasma. Thus fields transverse to the average Archimedean spiral geometry cannot exist in a quasi-stationary fashion. The magnetic field passing through the surface boundary between regions 2 and 3 is thus oriented in approximately the radial direction, and serves as a source for the interplanetary magnetic field.

It is this aspect of these models that will now be discussed. Figure 12 is a synoptic chart of the photospheric magnetic field obtained

by the Mount Wilson Observatory for Carrington solar rotation 1496. The dark gray regions represent magnetic field into the sun and the light gray regions represent magnetic field out of the sun. The contours of the magnetic field calculated on the source surface are shown superimposed. The solid contours represent magnetic field directed away from the sun, the dashed contours represent field toward the sun and the dotted contours represent the boundaries between regions of oppositely-directed fields. These contours also represent the current patterns that would exist near the "source" surface. At the bottom of the figure is a strip representing the sector pattern of the interplanetary magnetic field displaced by 5 days, the approximate transit time of the solar wind from the sun to the earth, and a graph of the interplanetary field magnitude. Toward-the-sun sectors are represented by heavy shading and away-from-the-sun sectors by light shading. A region of mixed polarity is represented by diagonal shading.

The smoothing of the photospheric field to a more sector like pattern on the source surface is evident. In the regions of the source surface where the field magnitude has reached the first contour level, the agreement with the direction of the interplanetary field is very good. The low magnitude of the interplanetary magnetic field from July 10 through July 14 may be related to the low field magnitude on the source surface at these times. On either side of this interval both the interplanetary field and the source surface fields have larger magnitudes. It is important to note that the photospheric field has scattered positive and negative fields over most ranges of longitudes but the field computed on the source surface has a smoothly varying field quite similar in many aspects to the interplanetary sector pattern field.

The large scale features of the photospheric field appear to persist to the source-surface and to be extended out by the solar wind. Correlations between the source surface field and the interplanetary magnetic field show definite peaks near 5 days time lag at all latitudes whereas the photospheric-interplanetary field correlated poorly at this time. Comparisons of eclipse observations with computed magnetic field structures by Altschuler and Newkirk and by Schatten suggest that the magnetic models, although not perfect, do provide a first order representation of the coronal and interplanetary magnetic field during quiet times. It has been recognized that flares can seriously disrupt the field patterns calculated.

The calculations of the coronal magnetic field allow the amount of non-radial flow or "nozzling" to be estimated. Schatten (1968) estimated a 1:6 area expansion beyond that expected for radial flow as that typical of sectors during the 1965-1966 period studied. The number calculated is not very accurate and probably varies significantly with time. However, the amount of "nozzling" calculated is not very large compared with the sunspot extension possibility, although it is certainly significantly different from a direct extension of the large scale field of the sun.

D. "Mean" Solar Field Observations and Suggested Interpretation

Recently observations of a "mean" solar field (the sun seen as a star) have been made using the Crimean solar telescope (Severny, 1969). The term "disk" field might have been a better notation for the observation as only the visible hemisphere of the sun contributes to the "mean" solar field. A comparison of this observation with the interplanetary magnetic field was undertaken by Severny et al. (1970). Figure 13 shows

their comparison. As can be seen, there is good agreement both in sign and magnitude. It is important to note that the interplanetary magnetic field is measured 4-1/2 days after the "mean" solar field to account for transport of the field from the sun to earth.

An interesting effect is that a cross-correlation between the two fields provides high peak at a lag of 4-1/2 days, as expected, but also a larger peak at 27 + 4-1/2 days. Schatten et al. (1969) found this same effect earlier in other work and attributed it to a delay of approximately one solar rotation between the appearance of a new magnetic feature in the photosphere and the resulting change in the interplanetary sector pattern.

Severny et al. note that their work implies that large areas on the sun (mostly outside of active regions) have a field whose predominant polarity agrees with the interplanetary magnetic field polarity. This is an important result in that it implies that sunspots and most flares do not affect the interplanetary field structure substantially. In fact, they find an inverse correlation of sign of the sunspot flux with the sign of the "mean" solar field.

The high correlation that Severny et al. (1970) have found suggests a prediction of the interplanetary field from "mean" solar field measurements. By observing the "mean" solar field in gauss and multiplying by 8, it should be possible to provide an approximate estimate of the interplanetary magnetic field in gammas either 4-1/2 days or 31-1/2 days in advance. Schatten (1970) has recently shown that the "mean" solar field-interplanetary field correlation may be explained from the coronal magnetic models. Figure 14 illustrates the manner in which the source surface model suggests the mean solar field-interplanetary field

correlation. The observed "mean" solar field is an average of the photospheric field over the solar disk with an appropriate weighting factor. This factor is a function of the angle from a position on the photosphere to the subsolar point. The main contribution to this factor is a result of the difference between the magnetograph measuring the line-of-sight magnetic field and the angular distribution of the photospheric field (perhaps radial on the average). Limb darkening and effects of sunspots (not seen by the magnetograph) are also contributing factors.

The source surface model implies that the interplanetary field near the earth results from the source surface field convected by the solar wind outward in about 4-1/2 days. Thus the field at the earth is the extended field from position A in Figure 14. The field at position A may be computed in this model as an integral of the photospheric field as follows:

$$\mathbf{B}_{INT} = \mathbf{B}_n \sqrt{2}\frac{R_s^2}{(215\,R_\odot)^2} = \frac{\sqrt{2}}{(215)^2}\frac{\int_{\text{sol. surf.}} \mathbf{B}_n (R_s/R_\odot)^2 M\, d\Omega}{\int_{\text{sol. surf.}} d\Omega}$$

$$= \frac{\sqrt{2}}{4\pi(215)^2}\int_0^\pi \mathbf{B}_n \left(\frac{R_s}{R_\odot}\right)^2 M\, 2\pi \sin\gamma\, d\gamma \qquad (9)$$

$$= \frac{\sqrt{2}}{2(215)^2}\int_0^\pi \mathbf{B}_{sf}(\text{weighting factor})\, d\gamma$$

where (weighting factor) =

$$-\sin\gamma (R_s/R_\odot)\left(1-\left(\frac{R_s}{R_\odot}\right)^2\right)\Big/\left(1+\frac{R_s^2}{R_\odot^2}-\frac{2R_s}{R_\odot}\cos\gamma\right)^{3/2}.$$

The quantity $\vec{B}_{INT}$ is the interplanetary magnetic field, $\vec{B}_n$ is the magnetic field at position A in Figure 14, $\vec{B}_{SF}$ is the solar field, R_s is the source surface radius and γ is the angle from any point in the photosphere to the subsolar point. This integral also has a weighting factor as a function of angle from the subsolar point and was shown to be quite similar to the mean solar field integral. Thus, the agreement between interplanetary field and the mean photospheric field is partly due to the fortunate coincidence between the source surface weighting factor and the integrated line-of-sight disk factor.

E. Active Regions-Influence of Flares

Active regions can influence the interplanetary magnetic field in one of two ways. The first way is through a rapid dynamic process whereby a flare occurring within an active region ejects a plasma outburst with resulting shock effects. This will be discussed here. The second is through the gradual evolutionary effect of the active region field upon the large-scale solar field accompanied by an evolving sector pattern. This will be discussed in the next section.

The first aspect suggested to Gold (1959) the possibility of magnetic tongues being ejected by active regions. Parker (1963) considered a blast wave model resulting in "kinked" azimuthally oriented fields due to the faster flare plasma. Taylor (1969) made a statistical study of shock surfaces and their relationship to solar flares. Figure 15 from Taylor shows the orientation of 8 probable shock surfaces relative to the flare position on the sun causing them. The dashed circle is a simplified picture of Hirshberg's (1968) large-scale shock structure. This line is an arc of a circle of radius 0.75 AU

centered on the 0^{o} line, 0.5 AU from the center of the sun. Many of the shock surfaces appear to be tangentially oriented to circles concentric with the one drawn. The shock surfaces imply that the radius of curvature of the shock front is less than, but of the order of 1 AU. All but shock surface 101a and 101b are consistent with the shock circle drawn. One of these, Taylor points out, is consistent with Gold's model and the other with Parker's. Needless to say, it would be beneficial to have several spacecraft widely separated in heliographic longitude to accurately determine the structure for individual events rather than relying on the statistical approach. Although shocks from flares appear to distort the plasma and magnetic field in a large region of space, they generally do so, only for a relatively short period of time.

F. Active Regions-Evolutionary Influence

The gradual evolutionary effect of the active regions upon the interplanetary magnetic field will now be discussed. Figure 16 from Wilcox and Colburn (1970) illustrates the evolutionary changes of the interplanetary magnetic sectors over six years. The observed sector structure is overlayed on the daily geomagnetic character index C9. Near solar minimum, with few active regions present, the sector structure was quasi-stationary. With the rise of solar activity, the sector patterns began to evolve more rapidly, changing with periods of a few months. New sectors are occasionally born and other decay away. Near the maximum of the solar cycle, there appear to be two large sectors per rotation. Wilcox and Colburn note that even approaching the maximum of the solar cycle, the interplanetary magnetic field retains the property that almost always several consecutive days have the same polarity.

Changes in the sector pattern are often related to the birth or decay of a sector. A classic example of the process will now be reviewed.

The birth of a sector was recorded in November 1965 and traced to the later stages in the evolutionary development of an active region. Figure 6 showing the magnetic loops, represents the birth of these new field lines in space. Figure 17 shows the history of this region as ascertained by Schatten et al. (1968). Each column represent a Carrington solar rotation and each row represents a particular form of observation. The top row is a schematic description of the interplanetary magnetic field structure, the third row represents the magnetograph observations, etc.

In the first solar rotation 1498, shown in Figure 17 one sees old background activity on the sun and toward-the-sun magnetic field present in the interplanetary medium and on the sun. In solar rotation 1499, the new activity is already present by the time the region appears at the east limb. At the central meridian passage of the region, sunspots, major flares, Type III radio bursts, and strong coronal Fe XIV emission have developed, together with an extensive plage and bipolar magnetic region. The interplanetary magnetic sector pattern has not been altered appreciably. In solar rotation 1500 magnetic loops appear in the interplanetary medium while strong 5303 emission and a bright plage remain. The bipolar magnetic feature on the sun appears to have grown larger and there is evidence of a North-South filament running through the plage.

During the next solar rotation, 1501, a quasi-static, away-from-the sun sector has developed in the interplanetary medium. This has been

accompanied by an elongation of the plage by differential rotation and a dispersal of the bipolar magnetic fields. It is interesting that the breakup of the bipolar group on the sun is associated with the formation of the away sector. The background magnetic field on the sun now appears to be oriented away from the sun.

The away sector is seen in the interplanetary medium in solar rotation 1502 as well. The first contour level on the magnetogram has been omitted in this rotation due to increased noise in the instrument, and thus the solar magnetic observations are less accurate here. Other forms of solar activity have subsided.

Calculations of the flux in the magnetic loops show that in the few days in which the loops were seen in interplanetary space, they transported all the flux in the solar bipolar region. Thus the probability of seeing such an event for each occurrence is about 10%. Thus it is fortunate that this event was observed during the birth process. Other similar events would not be expected to be so well documented. The solar bipolar region was unusual in that the background flux changed sign from toward-the-sun to away-from-the-sun following the breakup of the active region. Bumba and Howard (1965) have shown that most bipolar magnetic regions do not affect the photospheric background field. The amount of flux transported from the bipolar region agrees with the flux observed in the new sector formed. Thus the birth of a sector appears to be the aftermath of the magnetic loop formation process in the interplanetary medium and is related to a change in the background field polarity on the photosphere.

G. Interplanetary Field Near Solar Maximum

In this section several interplanetary magnetic field maps obtained near solar maximum are shown to illustrate the structural properties of the field due to solar activity.

The first solar rotation under discussion is Bartels' rotation 1843 (April 1968) shown in Figure 18. This rotation is one of those discussed by Severny et al. (1970) where the "mean" solar field correlated well with the interplanetary magnetic field. As is typical of many of the rotations under consideration by Severny et al., the field patterns shown are relatively smooth and obey the Archimedean spiral configuration quite well. The smooth field pattern is not related to any reduced amount of geomagnetic activity as shown by the indices C9 in Figure 16. This period appears relatively placid in terms of sector fields. Thus solar activity does not, at times, appear to influence the large-scale interplanetary magnetic field structure near 1 AU.

One region of interest in Figure 18 is the small 1-1/2 day wide sector of polarity toward-the-sun near day 101 (April 10) as shown in Figure 13, it correlates with a negative field pattern on the sun and hence may be classified as a "filament" of solar origin although it may be rather big for some definitions of "filament". It would be the smallest observed sector related to a solar feature, however. The distorted fields on days 112 and 113, probably represent some unknown field structures in space.

Figure 19 shows Bartels' rotation 1845 (June 1968). The first eight days of this rotation, still showing relatively placid field patterns, ended the studies of Severny et al. (1970). Of greater interest

here are the field patterns near days 180 and 174. These are similar to those one might expect for decaying sector fields. They are not, however, related to the disappearance of any of the sectors in which they occur. In fact, the positive sector near day 160, showing no such field patterns, disappeared a few rotations later.

There is an unusual kink in the field on day 178 that probably is not well represented in this map. Similarly, on day 175 there are fields directly opposed to each other. These are probably dynamic events of one sort or another with a rather complex structure. The high field strength, chaotic structure beginning near the end of day 162 occurs simultaneously with a geomagnetic storm. It is thus clear that at times the field is non-Archimedean.

Figure 20 shows Bartels' rotation 1849 (September-October 1968). This rotation is of interest in that it shows in one large portion, completely chaotic fields. On days 270 through 276, the field can by no means be represented by a simplified model. It would probably require at least several spacecraft separated in solar longitude, latitude and radial distance to attempt to unravel the field structures embedded in the solar wind on these days. Surprisingly, in the same Bartels' rotation, near day 263, there is a perfectly smooth sector boundary repeated 27 days later.

Figure 21 shows details of the sector structure for 1968 from Fairfield and Ness (1969). During the times when the field is twisted in a non-Archimedean structure or is of a filamentary nature, it often appears on this diagram as a small opposite polarity regions. As can be seen there are many such polarity filaments but they are rather limited in

time. In fact, although very few sectors can be found without them, they hardly confuse the sector pattern. This, I think, illustrates what may be the major effect of solar activity upon the interplanetary magnetic field: occasional disruptions in the smooth Archimedean field pattern. Further out in interplanetary space, the effects of these disturbances may be more pronounced with perhaps a significant influence on cosmic ray modulation. It is thus important to analyze the structure and evolution of these twisted field patterns. It will probably be necessary to utilize at least two spacecraft to disentangle the field structure.

H. Solar Cycle Variations

In addition to the changing sector patterns throughout the solar cycle, other properties of the interplanetary magnetic field are somewhat altered. Figure 22 from Wilcox and Colburn (1970) shows the synodic rotation rate of the interplanetary magnetic field as well as the sunspot number as a function of time. These authors point out that near sunspot minimum the rotation period was close to 27.0 days and that with the rise of new high - latitude solar activity in 1965 the interplanetary field recurrence period increased to about 28.0 days. The period then declined to 27.0 days near solar maximum. The authors suggest that the period will remain near 27.0 days until the increase of new sunspot activity near 1975. The data may be correlated not only with the period of the interplanetary field but perhaps also with the average latitude of the source of the field on the sun. This suggests the possibility that the source of the interplanetary field in the ecliptic is a low latitude source except when new activity is present and then the latitude is nearer 25°-30° heliographic latitude.

In addition to structural changes in the field pattern and recurrence period, the average interplanetary magnetic field strength is of interest. Hirshberg (1969) has looked at this question for a limited period and found no significant change. Figure 23 shows a more extensive analysis of the magnetic field magnitude distribution as a function of time. The top panel shows the field magnitude using hourly average IMP-1 data. The other panels utilize hourly average interplanetary field data from the Goddard Space Flight Center magnetometer experiments on Explorers 33, 34 and 35. Fairly complete coverage of the interplanetary magnetic field exists during these later years. As can be seen there is a small shift in the distribution towards higher field strengths as solar maximum is approached. The variability, however, is not as large as the sunspot number. The average field strength changes from about 4.5 gammas in 1963-4 and 1965 to about 6.2 gammas for 1967-1968. This is a 38% increase. A small part of this increase may be due to the field component averages being employed to compare field magnitudes in the IMP-1 and Explorer 33 analyses whereas in later results direct field magnitude averages were employed. Fairfield (1971) using IMP 3 observations and employing only component averages obtained at 4.6 gamma and 5.7 gamma field magnitude average for 1965 and 1966, respectively. This implies the observed variations in Figure 23 are real. The dashed line distribution for the IMP-1 time period from Ness et al. (1965) corresponds to the 3 hour field magnitude average computed from 5.46 minute field magnitudes rather than field components. The average is shown by the $<F_{3H}>$ symbol. The $<F_I>$ symbol represents the average instantaneous magnetic field from Ness (1970b) obtained at 20.5 second intervals.

It is interesting to compare these changes in the interplanetary field magnitude with the changes in the solar field magnitude. Figure 24 shows the large-scale solar magnetic field (Howard et al., 1967) near sunspot minimum (top) and near sunspot maximum (bottom). The top panel contour levels are 4, 8, 16, 24 and 50 Gauss and the bottom panel's levels are 5, 10, 20, 40 and 80 Gauss. Including the approximate 25% field magnitude increase in contour levels, and accounting for the data gap near 9/16/68, there is approximately twice as much photospheric flux at solar maximum as at solar minimum. This number is very uncertain due to the month to month variation in the solar field. Thus the 38% increase in interplanetary field magnitude although by no means insignificant is small compared with the crude estimate of a 100% increase in average photospheric field strength for the same period and the change in sunspot number from 10 to 110 throughout this solar cycle.

An examination of Figure 23 shows that the high field strength tail of the distribution is significantly enhanced. It appears that increased solar activity does not influence the field magnitude distribution very much but is associated with occasional enhancements in field strengths greater than 10 gamma. The percentage of the time that the field magnitude was greater than 10 gammas for each of the time periods in Figure 23 is shwon along with sunspot number in Figure 25. The vertical error bars along the 1963-4 result suggest variability due to different averaging methods. The I shows the effect of using instantaneous field magnitudes. The increase in this value is due to not averaging high field strengths with low ones. Surprisingly, the high field magnitudes

show variability similar to sunspot number. Although the spacecraft employed and the data processing are not identical throughout the years the results suggests that the magnitude enhancements are directly related to solar activity rather than differing data analyses. Many of the enhanced magnetic field magnitudes undoubtedly are also related to high speed streams and shocks occurrences in the solar wind which may be related to solar "events".

IV. Recent Developments, Problem Areas, and Future Work

A. Influence of Sun's Polar Fields on the Interplanetary Magnetic Field

Parker (1959) discussed the interplanetary magnetic field as an extension of the general solar field which he assumed to be a dipole for mathematical simplicity. The analyses of Wilcox and Ness (1965) and Schatten et al. (1969) related the interplanetary magnetic field polarities to the predominant polarity areas of the sun's background field. Their results showed that the predominant polarity areas of the sun were influencing the interplanetary field polarities in the ecliptic more than the polar fields of the sun were.

Recently, however, Rosenberg and Coleman (1969) have looked for an influence of the sun's dipole field upon the interplanetary magnetic field in the ecliptic. Figure 26 shows Wilcox's (1970a) extension of their analysis. The percentage of time of negative (i.e., directed toward-the-sun) interplanetary field polarity is plotted against time. A sine curve is fitted with a period of one year (shown). The resulting curve indicates a tendency for the interplanetary field to have negative polarity near the earth when the earth is at a positive heliographic latitude. This correlates with the sense of the sun's dipole field. Rosenberg (1970) suggests that this is not the influence of the observed high latitude polar field but rather an unobserved extension of the polar field to lower latitudes on the sun (ecliptic latitudes). Wilcox (1970a) has questioned the statistical significance of their result and provided additional data points (1968 and 1969 data) to their curve which do not add further support for their suggestion. Two or three more years

of data with a clear sense of the sun's polar field should provide a definite confirmation or rejection of the proposed effect.

B. Structure Out of Ecliptic Plane

Perhaps the most important aspect of the field out of the ecliptic plane is the three-dimensional average field structure. In accordance with Parker's (1963) model, the magnetic field would be directed along Archimedean spirals wound on cones with a half-angle corresponding to the heliographic co-latitude. This would result in away-from-the-sun sectors possessing an average northward directed field component (if represented in solar ecliptic coordinates) above the solar equator. The sign would reverse for toward-the-sun sectors in the opposite hemisphere.

Another aspect of the field out of the ecliptic plane is the percentage of time spent in away-from-the-sun or toward-the-sun sectors. In the ecliptic plane they occur nearly equally. A consequence of Rosenberg and Coleman's proposal, should it be correct, relates to the polarity of the interplanetary magnetic field out of the ecliptic plane. They fit the percentage negative polarity to a sine wave as a function of time, implying a direct relationship with heliocentric latitude. The relationship they obtain is such that approximately 70% of the time a negative polarity should occur when the earth is at 7.25° north heliographic latitude. Considering a 50% probability occurs at zero latitude, this implies that the field is directed toward the sun 100% of the time at only 18° north heliographic latitude. Obviously beyond this point the extrapolation of their result must end and in fact probably does so somewhat earlier. However, their rather large

effect for only 7.25° latitude implies that a point near 20° does have unidirected fields almost 100% of the time. The result is nearly the same if one chooses their effect to be proportional to the sine of the latitude. The unidirected field at 20° latitude could not relate directly back to the low latitude extension of the dipole photospheric fields as they suggest, because the observed photospheric field does not show only one polarity at 20° latitude. The unidirected polar fields on the sun begin at higher latitudes near the locations of the polar prominence zones (located at +70° and -55° latitude during 1968). These higher latitude fields still show occasional regions of opposite polarity, (Kotov and Stenflo, 1970). Thus the explanation of the extended sun's polar fields to low latitudes would seem implausible. Independent of the origin of these magnetic fields close to the sun, an extrapolation of Rosenberg and Coleman's analysis implies nearly unidirected fields at 20° heliographic latitude at 1 AU.

A different view is suggested by Wilcox (1970b) where the solar sector pattern of approximately equal and opposite fields occurs over a wide range of latitudes. Figure 27 shows a schematic of his model. A boundary exists approximately in the north-south direction. The pattern exists over a wide range of latitudes on both sides of the equator. The boundary rotates in an approximately rigidly rotating coordinate system. The solar sector pattern is the source of a corresponding interplanetary sector pattern. Thus if the Wilcox model is correct, in contrast to the Rosenberg and Coleman analysis, one would not expect to find much change in the polarity pattern of the interplanetary magnetic field out of the ecliptic until at least 40 or 50 degrees heliographic latitude.

My own thoughts would tend to lean towards compromise between the two. Perhaps a gradually increasing percentage polarity change would occur resulting in a nearly 100% unidirected field not at 18° but more typically at 30°, subject to fluctuations with time. The unidirected fields would occur at a lower latitude at times when the sun's polar fields were large (near solar minimum) and at higher latitudes when they were small (near solar maximum).

The coronal magnetic models might be related to this work. It is not necessary to require the sun's low latitude polar field to extend to ecliptic latitudes in order to explain Rosenberg and Coleman's observations. Figure 28 shows how polar fields, in accordance with the coronal models presented in Section II would provide a statistical influence on the field near the ecliptic. Some field lines, in the northern hemisphere, from the positive background field pattern would loop back to the northern polar fields thus freeing additional toward-the-sun magnetic flux and allowing it the possibility of extending to 1 AU at positive heliographic latitudes.

The other possibility mentioned in Section IV A is that the high latitude polar fields occasionally do extend to low latitudes at 1 AU. Figure 29 from Schatten (1968) shows the structure of the solar eclipse of June 30, 1954 near the minimum of the solar cycle. The drawing was prepared by Kiev astronomers from photographs taken at Kozeletsk, USSR. The long equatorial streamers and polar plumes are seen. In the bottom panel is shown the field structure that would result from the source surface model with no equatorial magnetic field. The important point

is that with high polar field values and low equatorial field strengths the polar fields appear to be able to reach to very low heliographic latitudes in the corona and presumably near 1 AU.

C. Hypothetical Interplanetary Field Structures

The interplanetary magnetic field may form rather unusual structures. Shown in Figure 30 are several possibilities that are of interest. The first three are structures previously discussed. Structure D is the inverse process of structure C whereby field lines near sector boundaries can decay away through a magnetic reconnection process close to the sun (inside of the Alfvén point). Additional closed field lines in the corona result, along with a "U" shaped interplanetary field pattern.

Structure E is similar to structure D in that magnetic fields are decaying. However, in structure E, the sector boundary itself may decay in many such closed magnetic field loops. This process may occur at 1 AU but may be more important further out in the interplanetary medium where it could result in the dissolution of the sectors. Structure F shows a small negative field polarity embedded within a positive sector. Such a filament may represent a "kink" convected past the spacecraft or may be of solar origin as shown here.

Structure G shows a schematic resulting from the work of Jokipii and Parker (1969). Solar cosmic ray diffusion suggested that interplanetary magnetic field lines would be "braided" due to the granular and super-granular motions on the sun causing the footpoints of the field lines to undergo a random-walk process. It might be possible to detect this "braiding" of field lines at 1 AU.

Structure H shows the "spaghetti" model proposed by McCracken and Ness (1966). Its main properties that distinguish it from some of the previous models are that "kinks" occur along a particular field line which is braided with other non-kinked fields and that the structures are discrete rather than continuous. If velocity perturbations in the solar wind are responsible for the kinks, one might expect all field lines in a particular region of space to be similarly distorted.

Structure I shows the ultimate effect of a non-uniform radially flowing solar wind. The dyadic velocity term, $\nabla \vec{V}$, which under a uniform flow results in the Archimedes spiral structure, now results in a "chaotic" field structure with the archimedes spiral being obeyed weakly. The magnetic field becomes oriented in an almost isotropic distribution.

D. Future Work

The important physical processes occurring in the solar wind plasma need to be tabulated and quantitatively treated. Their range of validity requires further study and they need to be brought together into a coherent entity. This concerns not only the large-scale field structure but the solar wind plasma as a whole: large-scale, small-scale, individual particle motions, waves, shocks, high speed streams, etc.

Many of the models discussed in this paper have received a certain amount of support but by no means have any of them been shown to be completely valid 100% of the time. Many of the interplanetary magnetic field structures shown in Section IV C need to be searched for. It will require much imaginative work, often with multiple satellite observations

in order to uniquely identify some of the field structures proposed (and to separate temporal effects properly).

Classifying the interplanetary field in terms of identified field structures rather than only "toward" or "away" sectors may aid our understanding of the relationship between the field and other phenomena. The relationship of these field structures to the sun needs further study as does the propagation of both galactic and solar cosmic rays within them. The geophysical effects of various structures may also be important. The variation of the interplanetary magnetic field needs to be more closely related to solar wind plasma parameters and to changing solar conditions. In addition, the relationship between microstructure and mesostructure within the solar wind needs study.

The magnetic field out of the ecliptic plane obviously requires observational work. Observations closer to the sun and further away from the sun than the earth, with a spacecraft located near earth as a monitor would also provide useful observations.

In the near future, Pioneers F and G will explore interplanetary space further away from the sun and Mariner-Venus-Mercury and HELIOS will explore closer to the sun than has any previous spacecraft. Thus much interesting work remains in future years concerning studies of the interplanetary magnetic field.

Acknowledgements

The author wishes to thank N. F. Ness, K. W. Ogilvie, D. H. Fairfield, R. P. Lepping, K. W. Behannon and J. E. Schatten from the Goddard Space Flight Center and J. M. Wilcox of the Space Sciences Laboratory for discussions concerning the material and scientific aspects of this paper.

This work was performed under the auspices of the National Aeronautics and Space Administration.

REFERENCES

Ahluwahlia, H. S. and A. J. Dessler, Diurnal variations of cosmic radiation intensity produced by a solar wind, Planetary Space Sci., 9, 195, 1962.

Altschuler, M. D., and G. Newkirk, Jr., Magnetic fields and the structure of the solar corona, Solar Physics, 9, 131 (1969).

Babcock, H. W. and H. D. Babcock, The sun's magnetic field, 1952-1954, Astrophys., J., 121, 349,.1955.

Biermann, L. Z., Kometenschweife und solare korpuscular strahlung, Z. Astrophys., 29, 274, 1951.

Bumba, V. and R. Howard, Large-scale distribution of photospheric magnetic fields, Astrophys. J., 141, 1502, 1965.

Burlaga, L. F., and N. F. Ness, Macro-and-micro-structure of the interplanetary magnetic fields, Canadian Journal of Physics, 46, 5962, 1968.

Coleman, P. J., Jr., and Rosenberg, R. L., The north-south component of the interplanetary magnetic field, Institute of Geophysics and Planetary Physics, Univ. of California at Los Angeles, Pub. 818, 1970.

Coleman, P. J., Jr., E. J. Smith, L. Davis, Jr., and D. E. Jones, The radial dependence of the interplanetary magnetic field: 1.0-1.5 AU, J. Geophys. Res., 74, 2826, 1969.

Coleman, P. J., Jr. and R. L. Rosenberg, The radial dependence of the interplanetary magnetic field: 1.0-0.7 AU, Trans. Am. Geophys. Union, 49, 727, 1968.

Davis, L. Jr., E. J. Smith, P. J. Coleman, Jr., and C. P. Sonett, Interplanetary magnetic measurements, The Solar Wind, Ed. by Mackin and Neugebauer, Pergamon Press, London, p. 35, 1964.

Davis, L., Jr., Mariner II observations relevant to solar fields, Stellar and Solar Magnetic Fields, p. 202, Ed. R. Lüst, North-Holland, Amsterdam, 1965.

Fairfield, D. H., private communication (1971).

Fairfield, D. H., K. W. Behannon and N. F. Ness, Interplanetary magnetic field polarity: 1966-1968, Trans. Am. Geophys. Union, pg. 300, 1969.

Fairfield, D. H. and N. F. Ness, Magnetic field measurements with the IMP 2 satellite, J. Geophys. Res., 72, 2379, 1967.

Gold T., Plasma and magnetic fields in the solar system, J. Geophys. Res., 64, 1665, 1959.

Hirshberg, J., The transport of flare plasma from the sun to the earth, Planetary Space Sci., 16, 309, 1968.

Hirshberg, J., Interplanetary magnetic field during the rising part of the solar cycle, J. Geophys. Res., 74, 5814, 1969.

Howard, R., V. Bumba, and S. F. Smith, Atlas of solar magnetic fields, Carnegie Institute of Washington Publication 626, 1967.

Hundhausen, A. J., Interplanetary shock waves and the structure of the solar wind disturbances, these proceedings, 1971.

Jokipii, G. and E. N. Parker, Stochastic aspects of magnetic lines of force with application to cosmic ray propagation, Astrophys. J., 155, 777, 1969.

Kotov, V. A. and J. O. Stenflo, A comparison of simultaneous measurements of the polar magnetic fields made at Crimea and Mount Wilson, Solar Physics, 15, 265-272, 1970.

McCracken, K. G., and N. F. Ness, The collimation of cosmic rays by the interplanetary magnetic field, J. Geophys. Res., 71, 3315, 1966.

Ness, N. F., C. S. Scearce and J. B. Seek, Initial results of the IMP 1 magnetic field experiment, J. Geophys. Res., 69, 3531, 1964.

Ness, N. F., The Magnetic structure of interplanetary space, Proceedings of the XI International Conference on Cosmic Rays (invited papers and rapporteur talks). Publ. by Central Research Institute of Physics of the Hungarian Academy of Sciences, Budapest, p. 41, 1970b.

Ness, N. F. C. S. Scearce, J. B. Seek and J. M. Wilcox, A summary of results from the IMP-1 magnetic field experiment, GSFC preprint X-612-65-180, 1965.

Ness, N. F., Magnetometers for space research, Space Science Reviews, 11, 459-554, 1970a.

Ness, N. F. and J. M. Wilcox, Solar origin of the interplanetary magnetic field, Phys. Rev. Letters, 13, 461, 1964.

Parker, E. N., Dynamics of the interplanetary and magnetic fields, Astrophys. J., 128, 664, 1958.

Parker, E. N., Interplanetary Dynamical Processes, Interscience, New York, 1963.

Rosenberg, R. L., and P. J. Coleman, Jr., Heliographic latitude dependence of the dominant polarity of the interplanetary magnetic field, J. Geophys. Res., 74, 5611, 1969.

Rosenberg, R. L., Unified theory of the interplanetary magnetic field, Solar Physics, 15, 72, 1970.

Schatten, K. H., A "source surface theory" corollary: The mean solar field-interplanetary field correlation, Solar Physics, 15, 499-503, 1970.

Schatten, K. H., Large-scale configuration of the coronal and interplanetary magnetic field, Thesis, Univ. of California, Berkeley, 1968.

Schatten, K. H., N. F. Ness and J. M. Wilcox, Influence of a solar active region on the interplanetary magnetic fields, Solar Physics 5, 240-256, 1968.

Schatten, K. H., J. M. Wilcox and N. F. Ness, A model of coronal and interplanetary magnetic fields, Solar Physics, 9, 442-455, 1969.

Severny, A., Nature, 224, 53, 1969.

Severny, A., J. M. Wilcox, P. H. Scherrer, and D. S. Colburn, Comparison of the mean photospheric magnetic field and the interplanetary magnetic field, Solar Physics, 15, 3, 1970.

Taylor, H. E., Sudden commencement associated discontinuities in the interplanetary magnetic field observed by IMP 3, Solar Physics, 6, 320, 1969.

Wilcox, J. M., A. D. Ritchie and N. F. Ness, Movie of the interplanetary magnetic field, Space Sciences Lab. University of California at Berkeley, Series 7, issue 53, 1966.

Wilcox, J. M., Statistical significance of the proposed heliographic latitude dependence of the dominant polarity of the interplanetary magnetic field, J. Geophys. Res., 75, 2587-2590, 1970a.

Wilcox, J. M., The extended coronal magnetic field, to be published in the Proceedings of NATO Advanced Study Institute, Athens, 1970b.

Wilcox, J. M. and D. S. Colburn, Interplanetary sector structure in the rising portion of the sunspot cycle, J. Geophys. Res., 75, 6366, 1970.

Wilcox, J. M. and N. F. Ness, Quasi-stationary corotating structure in the interplanetary medium, J. Geophys. Res., 70, 5793, 1965.

Wilcox, J. M., The interplanetary magnetic field: solar origin and terrestrial effects, Space Sci. Rev., 8, 258, 1968.

FIGURE CAPTIONS

Figure 1 Projection onto the solar equatorial plane of the lines of force of any solar field which is carried away from the sun by outward-streaming gas with a velocity of 10^3 km/sec.

Figure 2 Scatterplot of the radial and azimuthal interplanetary magnetic field component changes from Mariner 2. The dashed line shows the expected average for theoretical spiral field lines from the sun.

Figure 3 The + and - signs along the circumference of this figure indicate the direction of the measured interplanetary magnetic field during successive three hour intervals. Parentheses indicatee times when the field direction is substantially displaced from the spiral angle. The inner portion of the figure is a schematic representation of the sector structure of the interplanetary magnetic field suggested from the IMP 1 observations

Figure 4 Interplanetary magnetic field and cosmic ray anisotropy on December 30, 1965 from Pioneer 6 observations. The interplanetary magnetic field shows a "kink" structure which is also seen in the cosmic ray anisotropy directions.

Figure 5 Extrapolated ecliptic magnetic field pattern during Bartels' solar rotation number 1784, prepared from IMP-1 magnetic field measurements. The gaps in the circle at 1 AU and in the data represent times when the satellite is near perigee and unable to sample the interplanetary medium. The tick

marks at 1 AU indicate the amount of solar rotation during one day. The interval between the tick marks is labeled with the date of observation. The line drawn at the bottom of the figure separates observations 27 days apart. The observations extend from November 28, 1963 through December 25, 1963.

Figure 6 Enlargement of the magnetic flux loops observed near day 310, 1965. The dip in the field pattern on day 308 has associated with it a strong northward field.

Figure 7 Averages over 27 days of $B_{\theta+}$, $B_{\theta-}$, $B_{\theta S}$ $b_{\theta+}$ and Kp for the interval covered by the Mariner 4 data. The solid curve drawn in the $B_{\theta S}$ panel represents a best fit to $B_{\theta S}$ with a function proportional to heliographic latitude..

Figure 8 Average interplanetary magnetic field components as a function of radial distance from the sun. The dashed line is that magnitude expected for an Archimedes spiral field geometry. Each point is a 29 day average.

Figure 9 Joint distributions of pairs of component variables from measurements taken near 1.5 AU, Bartels' solar rotation 1804, May 22-June 17, 1965.

Figure 10 Mean values of the magnitudes of various components used to describe the interplanetary magnetic field versus time, heliocentric range (AU) and solar latitude (degrees). B is field magnitude; B_L is the projection of the field on the $r\phi$ plane and B_p is the projection of the field on the $\theta\phi$ plane. Averages were taken over periods of one rotation of the sun. The time assigned to each solar rotation is the time of the middle of the

rotation period. The smooth curves are values expected for an ideal spiral field. Averages of Ap, the daily sum of Kp, and the mean neutron intensity at Climax are also plotted.

Figure 11 Schematic representation of the source surface model. The photospheric magnetic field is measured in Region 1 at the Mt. Wilson Observatory. Closed field lines(loops) exist in Region 2. The field in this region is calculated from potential theory. Currents flowing near the source surface eliminate the transverse components of the magnetic field and the solar wind extends the source surface magnetic field into interplanetary space. The magnetic field is then observed by spacecraft near 1 AU.

Figure 12 A synoptic chart of the photospheric magnetic field obtained by the Hale Observatory on Mount Wilson for Carrington solar rotation 1496. The dark gray regions represent magnetic field into the sun, the light gray regions magnetic field out of the sun. The contour levels are 6, 12, 20 and 30 gauss. Contours of the magnetic field on the source surface are shown. Dashed contours represent field directed towards the sun and solid contours, field directed away from the sun. Dotted contours represent regions of zero field. Contour levels are 0.25 and 0.75 gauss. Also shown at the bottom of the figure are the interplanetary sector structure and magnetic field magnitude displaced by 5 days. Toward sectors are represented by heavy shading, away sectors by light shading, and mixed polarity fields by diagonal shading.

Figure 13 Comparison of the magnitude of the "mean" solar field and of the interplanetary field. The open circles are the daily observations of the mean solar field, and the dots are 3-hour average values of the interplanetary field magnitude observed near the earth. The solar observations are displaced by 4-1/2 days to allow for the average sun-earth transit time. The abscissa is at the time of the interplanetary observations.

Figure 14 Relationship between the mean solar field, the source surface field, and the interplanetary field. The mean solar field is a weighted average of the disk field (indicated by the shading). The source surface field is the magnetic field on the source surface, position A. This is computed from a weighted average of the photospheric field, quite similar to the mean solar field. The solar wind convects this field to the earth in about 4-1/2 days while solar rotation twists the field to approximate an Archimedes spiral as shown.

Figure 15 A plot of the orientation of 8 probable shock surfaces at the appropriate heliocentric longitude relative to the flare. The dashed line is an arc of a circle of radius 0.75 AU centered on the 0° line 0.5 AU from the sun.

Figure 16 Observed sector structure of the interplanetary magnetic field, overlayed on the daily geomagnetic character index C9, as prepared by the Geophysikalisches Institut in Göttingen. Light shading indicates sectors with field predominantly away from

the sun. Diagonal bars indicate an interpolated quasi-stationary structure during 1964.

Figure 17 Chart showing the history of the active region associated with the interplanetary magnetic loop event. Each column shows the development of the feature during successive solar rotations. Each row describes different observations of the region. The figures are centered on the central meridian plage passage with the Mount Wilson magnetograph observations and the Fraunhofer Institute maps extending over a scale of 40° in longitude and 20° in latitude. The first contour level on the Mount Wilson magnetogram for solar rotation 1502 has been omitted due to an increase in noise during that time period. The plage area is graphed on a scale of millionths of the solar disk.

Figure 18 Interplanetary magnetic field map for Bartels' rotation 1843. The field patterns are similar to those observed by IMP-1 although the period is close to solar maximum.

Figure 19 Interplanetary magnetic field map for Bartels' rotation 1845. This figure shows looped field lines (near days 180 and 174) which appear to be in the process of being transported out of the interplanetary medium by the solar wind. This process may be related to sector decay.

Figure 20 Interplanetary magnetic field for Bartels' rotation 1849. Note the completely chaotic field structure at the top of the figure.

Figure 21 Interplanetary magnetic sector structure for 1968 overlayed on chart of planetary magnetic three-hour-indices Kp (after Bartels). The heavy shading represents magnetic field away-from-the-sun, and the light shading, field toward-the-sun.

Figure 22 Synodic rotation period of the interplanetary magnetic field and sunspot number as a function of time.

Figure 23 Interplanetary magnetic field magnitude distribution as a function of time. Average field magnitude is shown by the symbols. Somewhat different data processing has occurred throughout the years discussed in the text. Note the change from 1965 to 1966.

Figure 24 Two synoptic charts of the photospheric magnetic field obtained by theHale Observatory on Mount Wilson. One rotation is obtained near sunspot minimum (top) and one near solar maximum (bottom). There is a data gap near the center in the lower panel. The heavy shading indicates into-the-sun magnetic field and the light shading, out-of-the-sun field. The contour levels on the top panel are 4, 8, 16, 24 and 50 gauss and on the bottom, they are 5, 10, 20, 40 and 80 gauss.

Figure 25 Percentage time the hourly average interplanetary magnetic field magnitude exceeds 10 gammas and unspot number as a function of time in years. The enhanced field magnitudes appear to be related to enhanced sunspot number and thus possibly to solar activity. The I refers to the instantaneous field exceeding 10 gammas.

Figure 26 Interplanetary field polarity observed by spacecraft having nearly the earth's heliographic latitude. For each solar rotation period the lower bar is the actual number

of days of negative polarity. The upper bar is 27 minus the number of days of positive polarity. The distance between the bars is the number of days of missing data. The sine function is the least-squares, best-fit function to the data (9.1% rms deviation) with a one year period. The data for solar rotation periods 1795 through 1840 were used. This function is $50.9 - 17.6 \sin(\omega t - 0.171)$, where t is measured in terms of Bartels' solar rotations. This function leads by only 5° the heliographic latitude of the earth, $\beta(t) = -.73^{\circ} \sin(\omega t - 0.085)$. Some of the Mariner 4 and Pioneer 6 data were taken at latitudes differing somewhat from that of the earth.

Figure 27 A schematic of Wilcox's average position of a solar sector boundary during 1965. On each side of the boundary the weak background photospheric magnetic field is predominantly of a single polarity in equatorial latitudes on both sides of the equator. This solar sector extends to latitudes near 40 or 50 degrees.

Figure 28 Schematic showing how polar fields can cause coronal magnetic loops to form which will influence the statistical distribution of toward-and away-from-the-sun sectors at 1 AU with respect to heliographic latitude. Shaded areas represent out-of-the-sun magnetic field. In the northern hemisphere, coronal loops form allowing some magnetic flux to leave the positive (out-of-the-sun) magnetic regions and be directed into the negative polar field. This allows some negative flux to extend to 1 AU

north of the solar equatorial plane. The situation is reversed in the southern hemisphere. This process allows Rosenberg and Coleman's hypothesis to be extended to higher latitudes and yet be consistent with the polar field being confined to the suns' polar regions as observed.

Figure 29 Drawing of the corona at the June 30, 1965 eclipse near solar minimum (Vsekhsvjatsky, 1963) (top). Appearance of the field line configuration in the corona using the "source surface" model with only polar fields present in the photosphere (bottom). These drawings show how the sun's polar field may extend to lower heliographic latitudes with increasing radial distance in the corona and the solar wind.

Figure 30 Schematic showing nine types of interplanetary magnetic field structures. The three in the first row have rather strong observational support. The remaining six are suggested field patterns that may occur but probably require several spacecraft or detailed observations to identify. Future work should be devoted to examining and classifying the observed interplanetary magnetic field according to these structures.

Table 1

Starting time UT			End time UT			V_{start} km/sec	V_{end} km/sec	φ spiral angle	$1 - \frac{\Delta V}{V} \frac{27.5}{\Delta t + (2\pi)}$	φ azimuthal velocity gradient	φ observed
0300	343	63	0300	344	63	435	283	130°	- .85	50°	48°
2100	351	63	2100	352	63	305	215	301°	-1.08	223°	227°
0000	011	64	0000	015	64	493	210	310°	.11	276°	273°
1500	033	64	1500	034	64	378	307	129°	.07	94°	53°
2100	037	64	2100	038	64	460	350	314°	-.2	259°	244°
2100	001	64	2100	002	64	310	490	133°	3.0	162°	145°

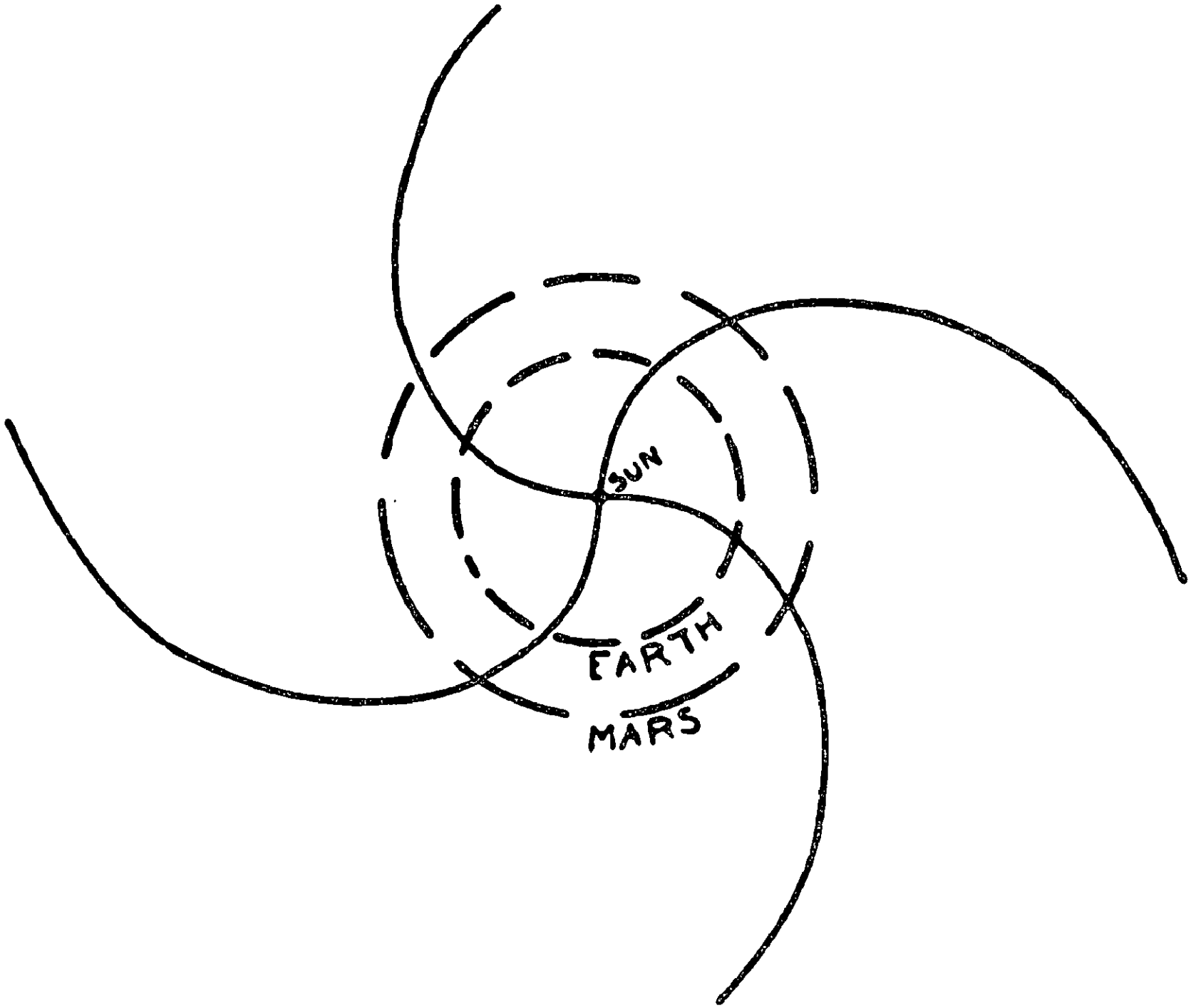

FIGURE 1

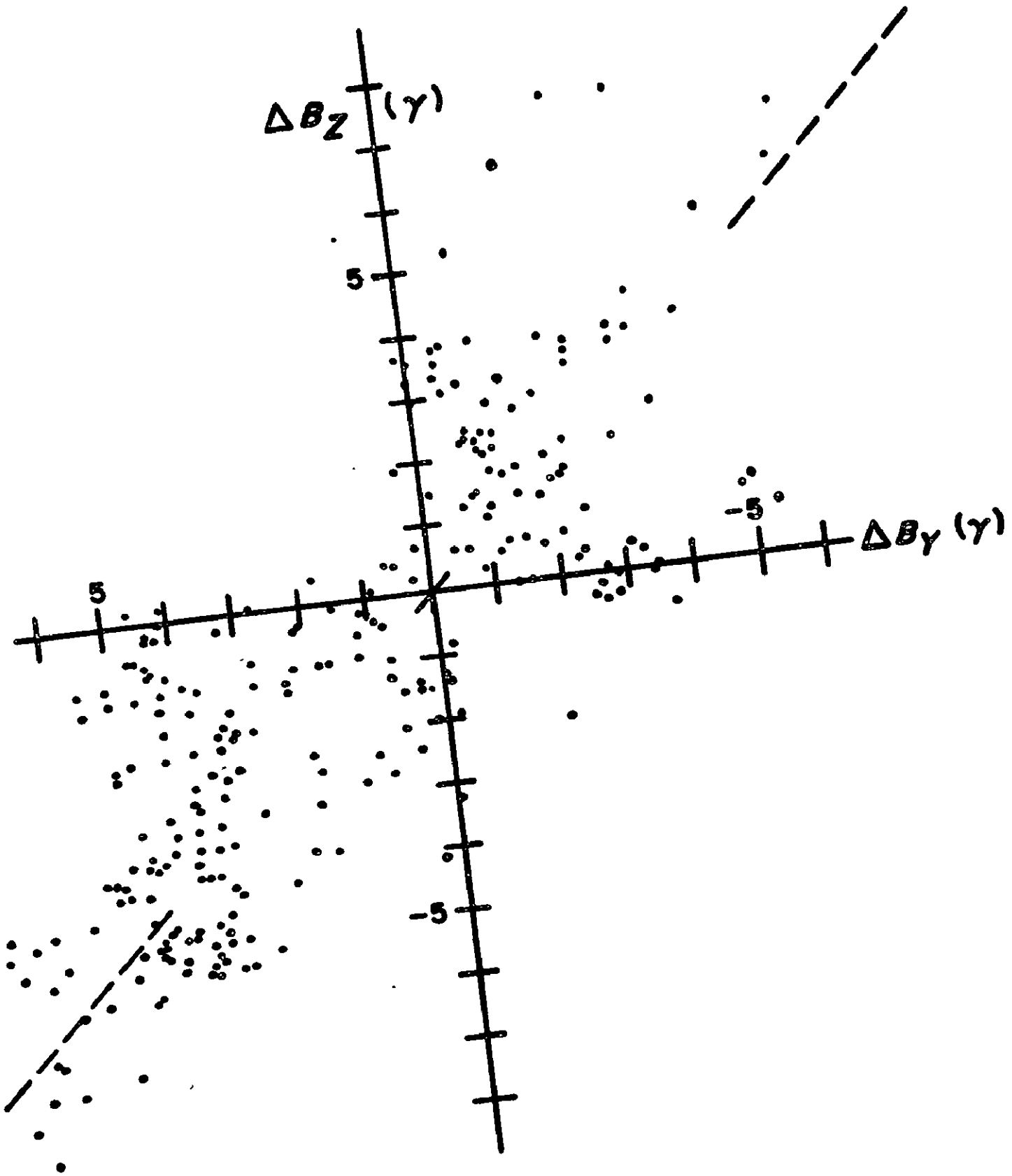

FIGURE 2

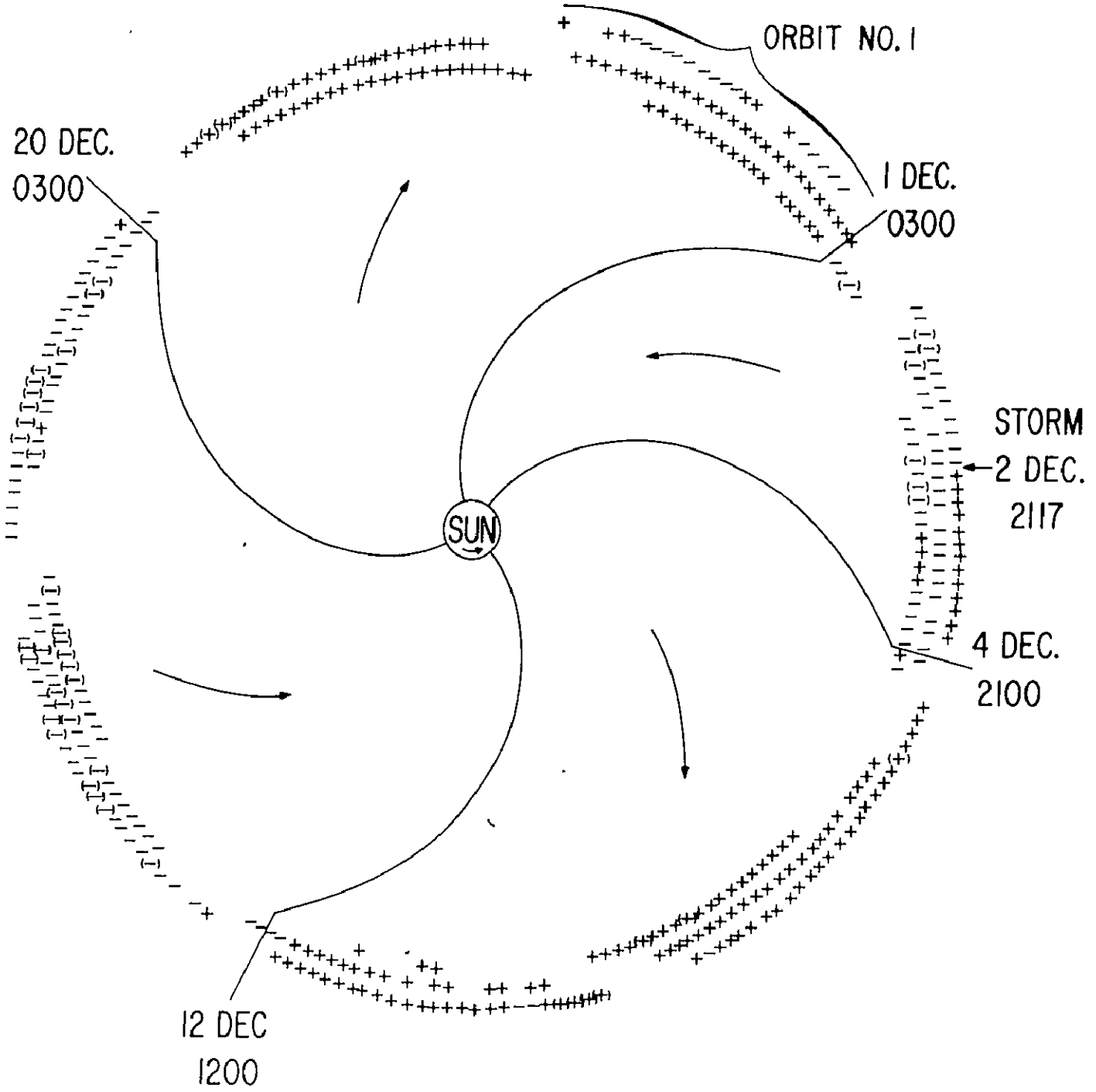
ORBIT NO. 1
20 DEC.
0300
1 DEC.
0300
STORM
2 DEC.
2117
SUN
4 DEC.
2100
12 DEC
1200

FIGURE 3

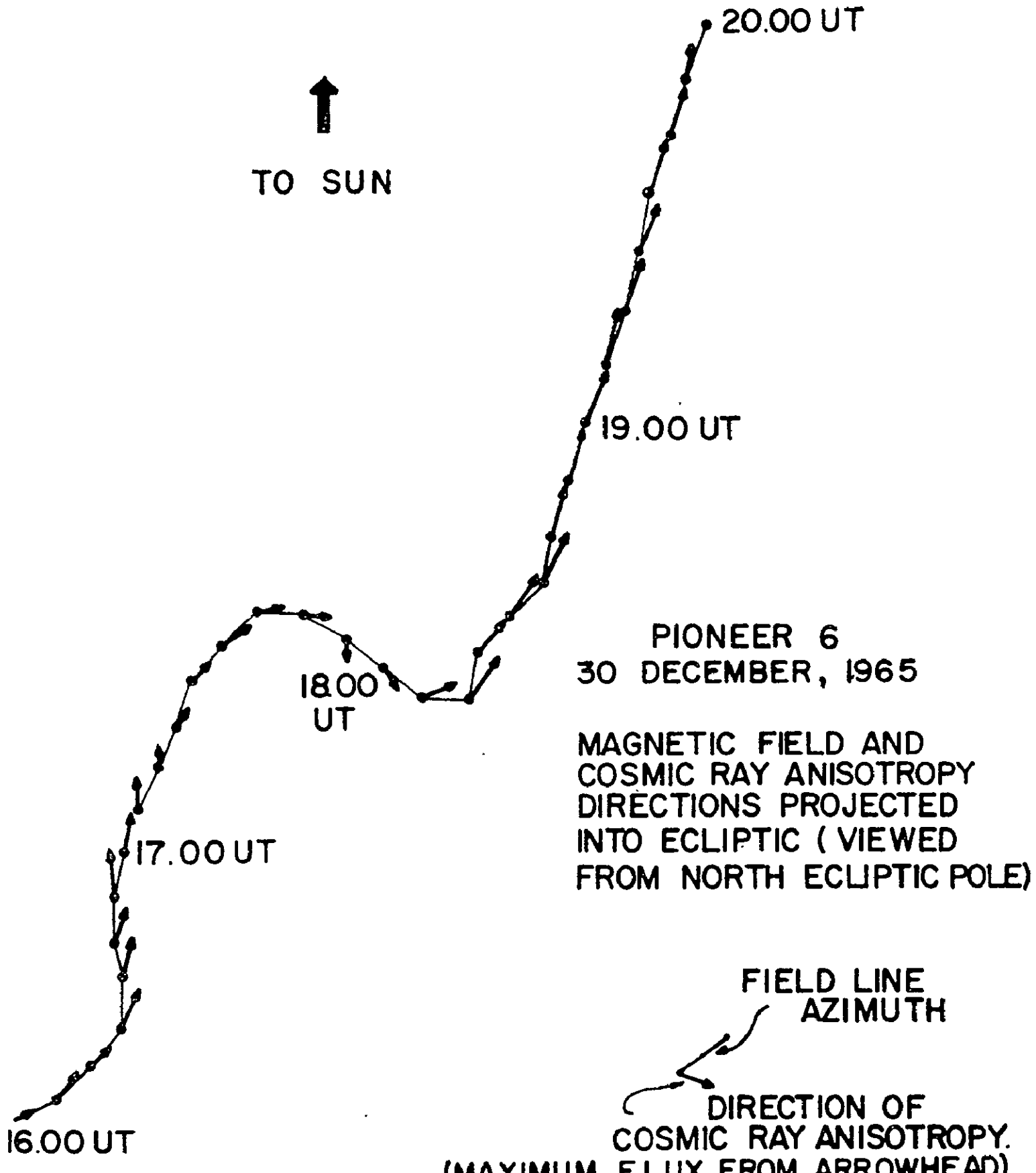
20.00 UT
TO SUN
19.00 UT
18.00
UT
17.00 UT
16.00 UT
PIONEER 6
30 DECEMBER, 1965
MAGNETIC FIELD AND
COSMIC RAY ANISOTROPY
DIRECTIONS PROJECTED
INTO ECLIPTIC (VIEWED
FROM NORTH ECLIPTIC POLE)
FIELD LINE
AZIMUTH
DIRECTION OF
COSMIC RAY ANISOTROPY.
(MAXIMUM FLUX FROM ARROWHEAD)

FIGURE 4

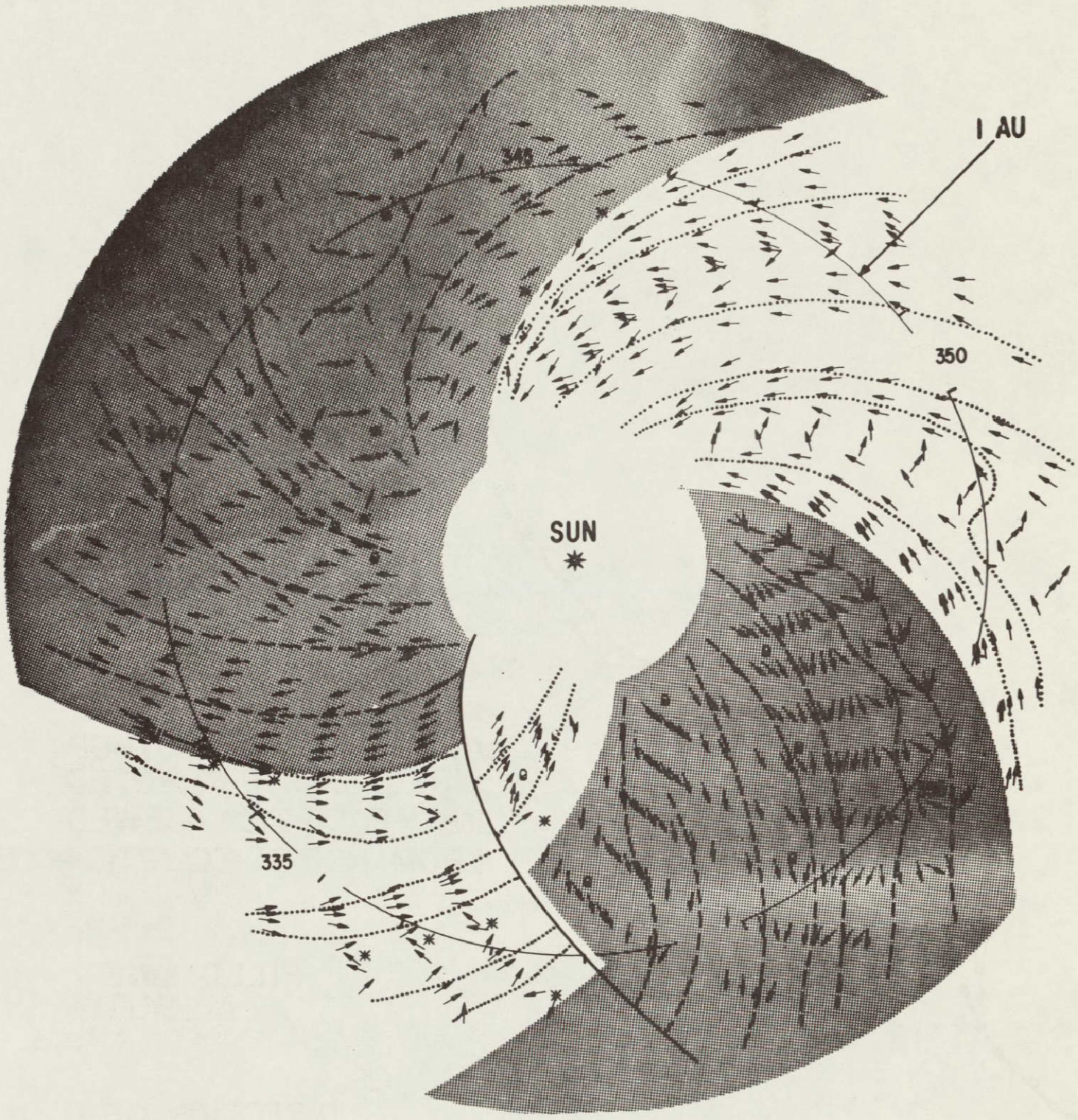

FIGURE 5

⊕2

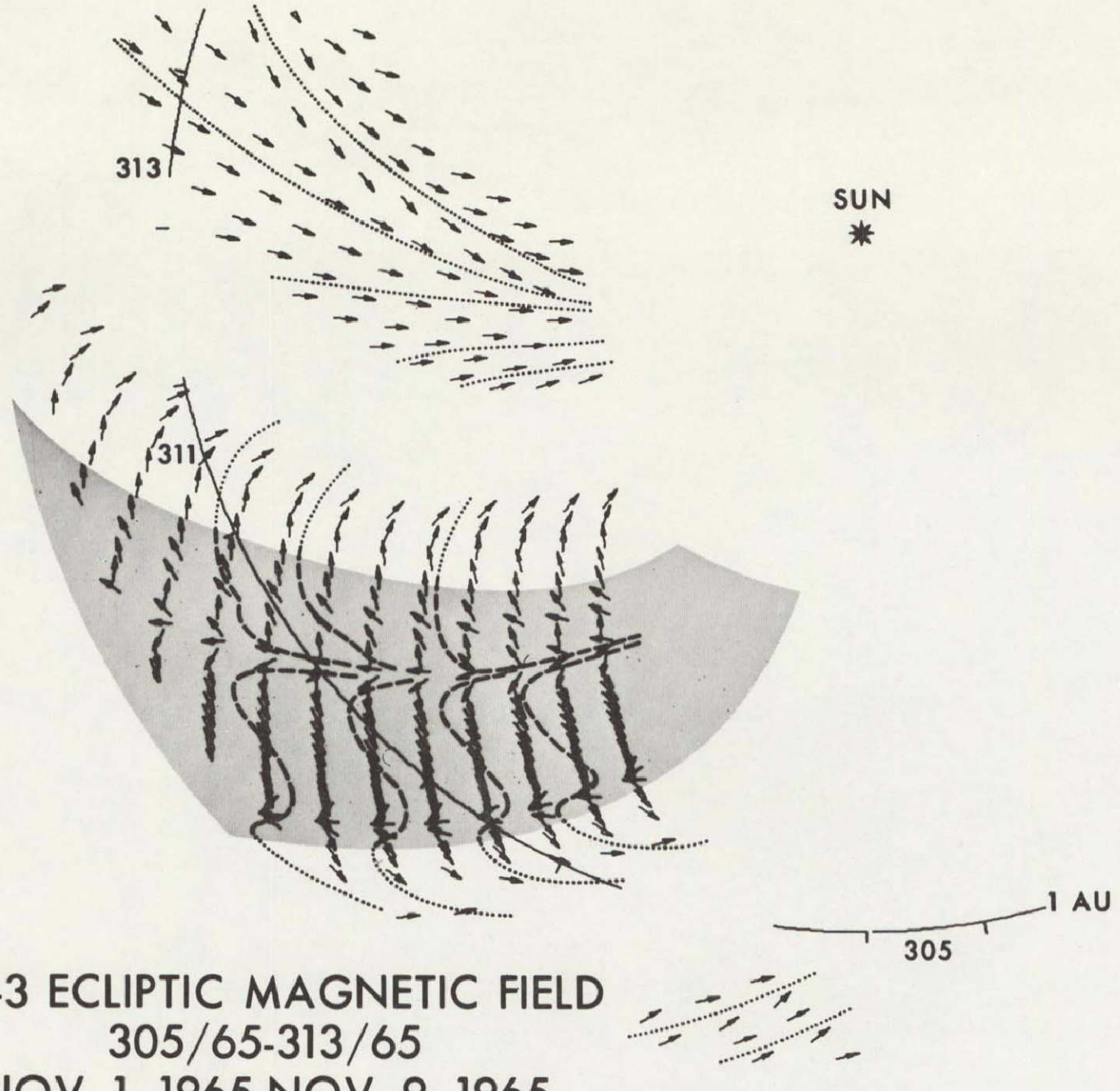

IMP-3 ECLIPTIC MAGNETIC FIELD
305/65-313/65
NOV. 1, 1965-NOV. 9, 1965

FIGURE 6

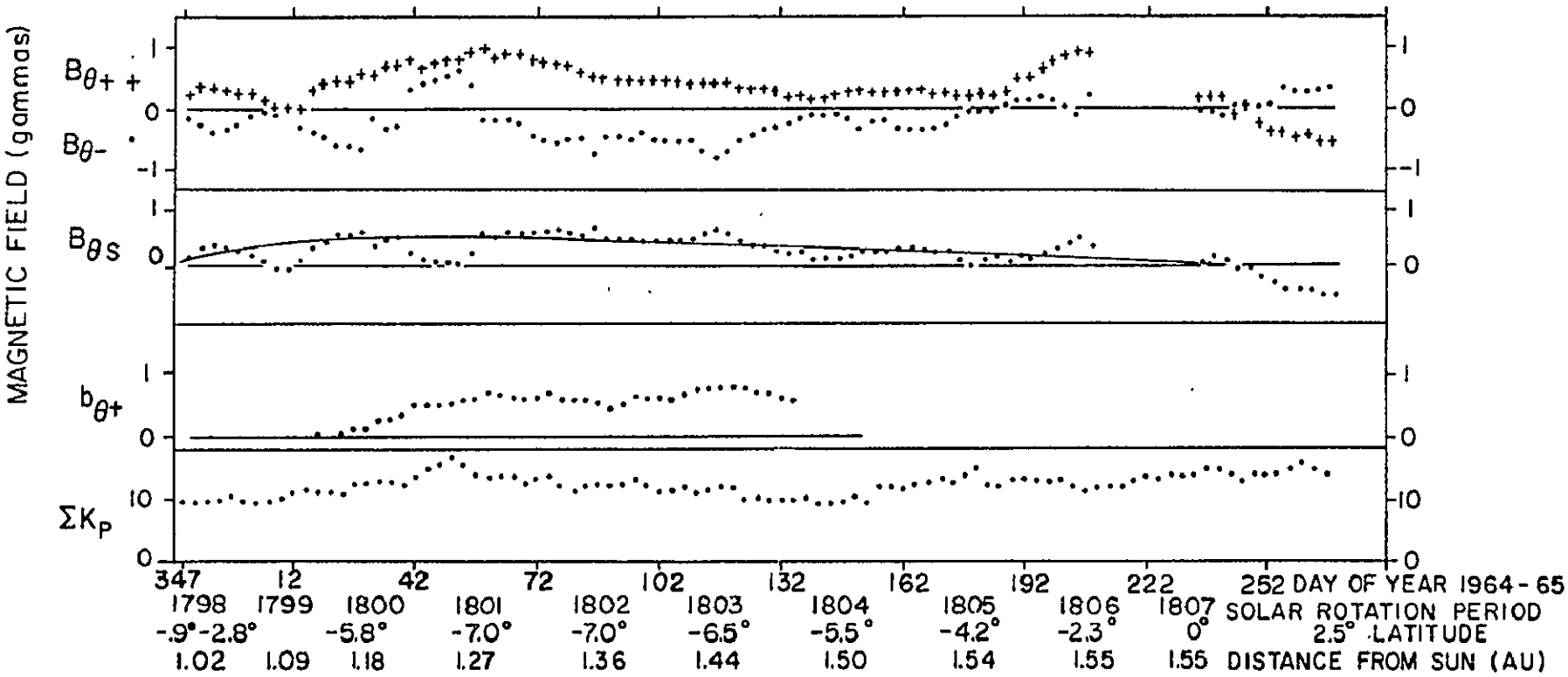

MARINER 4

OVERLAPPING 27 DAY AVERAGES

$B_{\theta+}$ is $\bar{B}_\theta$ for $B_r \geq 0$, $B_{\theta-}$ is $\bar{B}_\theta$ for $B_r < 0$, $B_{\theta S} = (B_{\theta+} - B_{\theta-})/2$

$b_{\theta+} = -\sqrt{4\pi\rho}\, v_\theta$

FIGURE 7

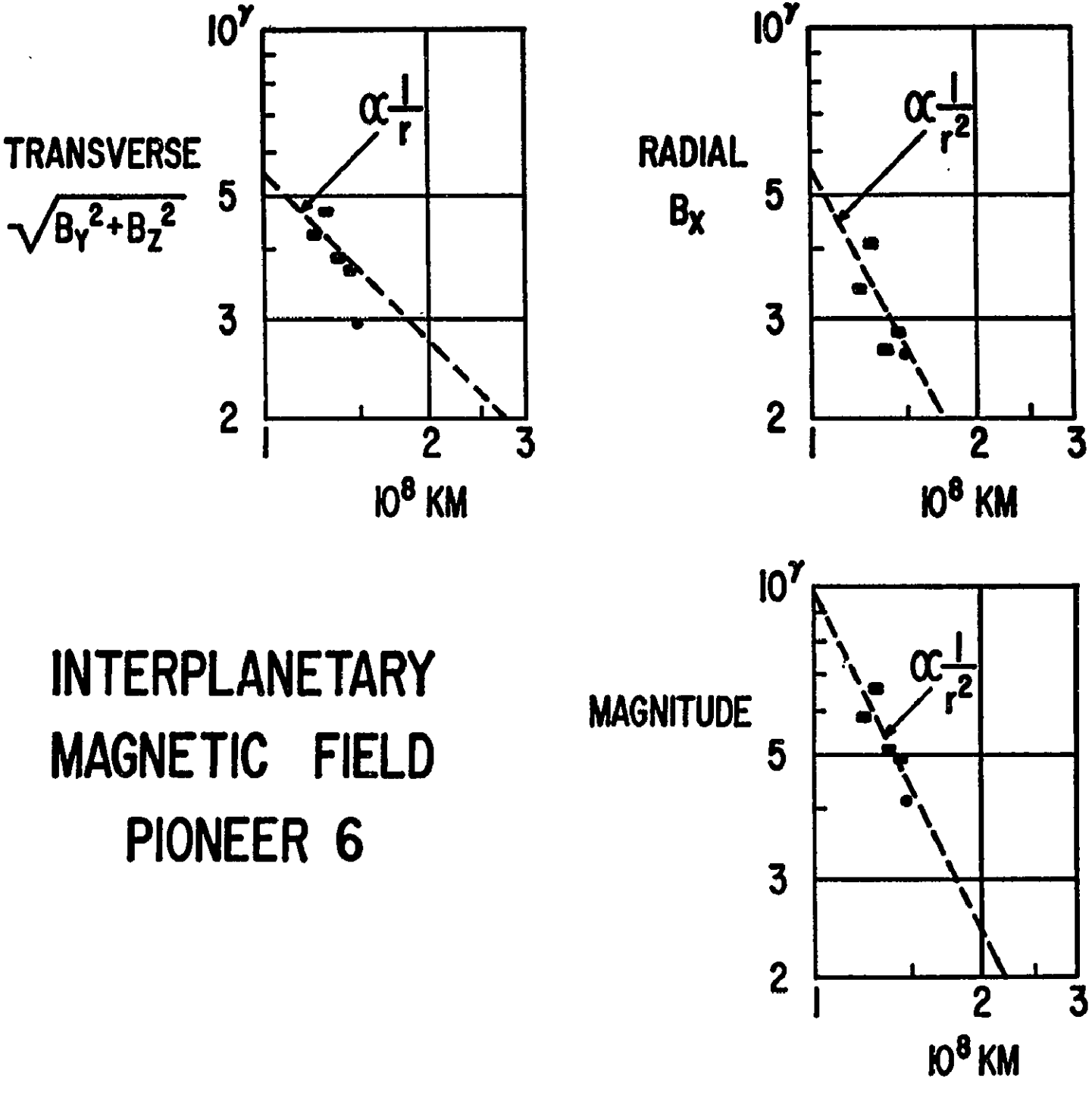
TRANSVERSE
$\sqrt{B_Y^2+B_Z^2}$
10^γ
5
3
2
$\propto \frac{1}{r}$
1
2
3
10^8 KM
RADIAL
B_X
10^γ
5
3
2
$\propto \frac{1}{r^2}$
1
2
3
10^8 KM
INTERPLANETARY
MAGNETIC FIELD
PIONEER 6
MAGNITUDE
10^γ
5
3
2
$\propto \frac{1}{r^2}$
1
2
3
10^8 KM

FIGURE 8

MARINER 4

INTERPLANETARY MAGNETIC FIELD JOINT DISTRIBUTIONS

SR NO. 1804, 22 MAY - 17 JUN, 1965

$\bar{r}$ = 1.50 AU, $\bar{\theta}$ = 95.2°, $\bar{\beta}$ = -5.2°

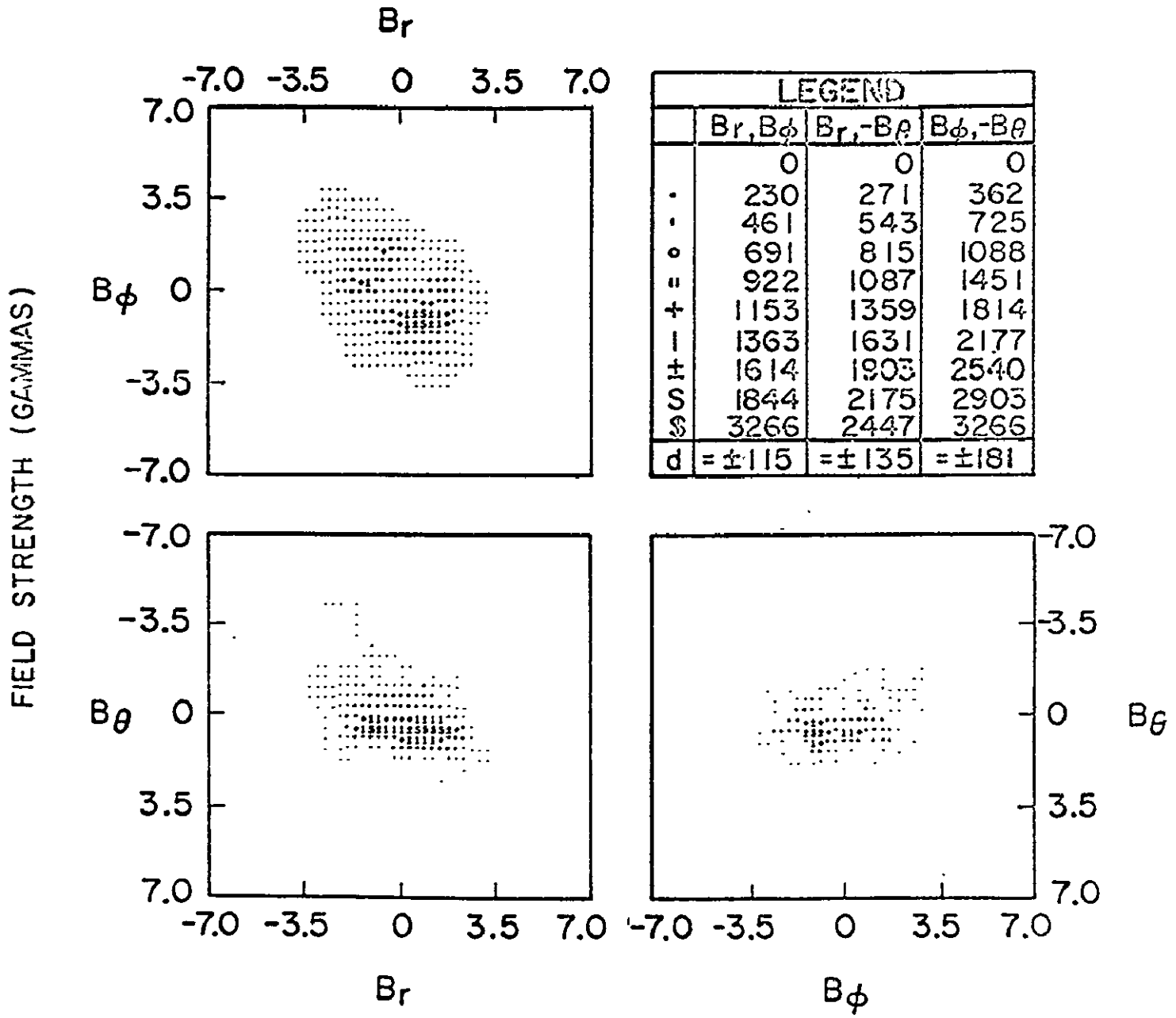

FIGURE 9

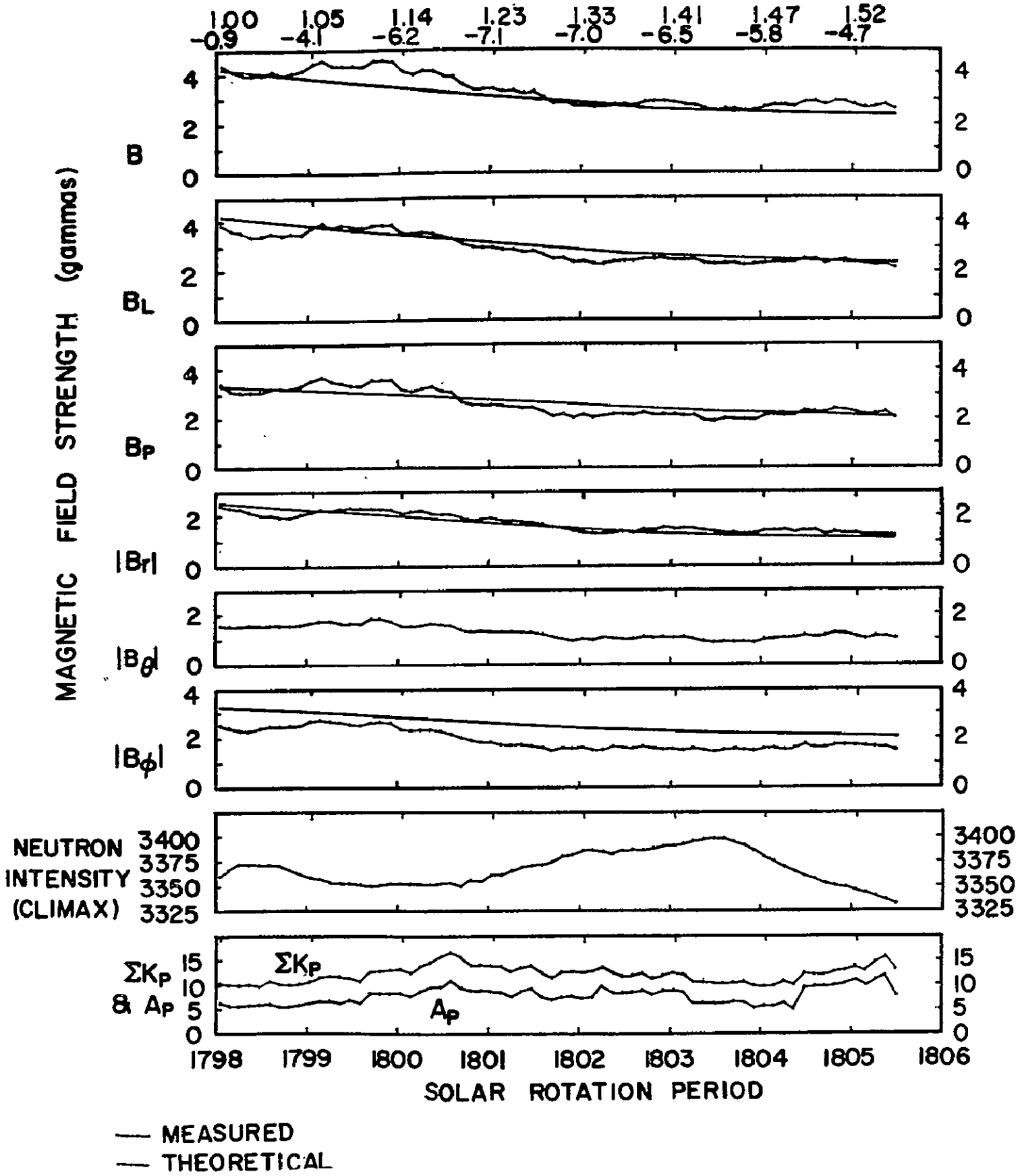
1.00 1.05 1.14 1.23 1.33 1.41 1.47 1.52
-0.9 -4.1 -6.2 -7.1 -7.0 -6.5 -5.8 -4.7
MAGNETIC FIELD STRENGTH (gammas)
B
BL
BP
|Br|
|Bθ|
|Bφ|
NEUTRON INTENSITY (CLIMAX)
3400 3375 3350 3325
ΣKP & AP
ΣKP
AP
1798 1799 1800 1801 1802 1803 1804 1805 1806
SOLAR ROTATION PERIOD
— MEASURED
— THEORETICAL

FIGURE 10

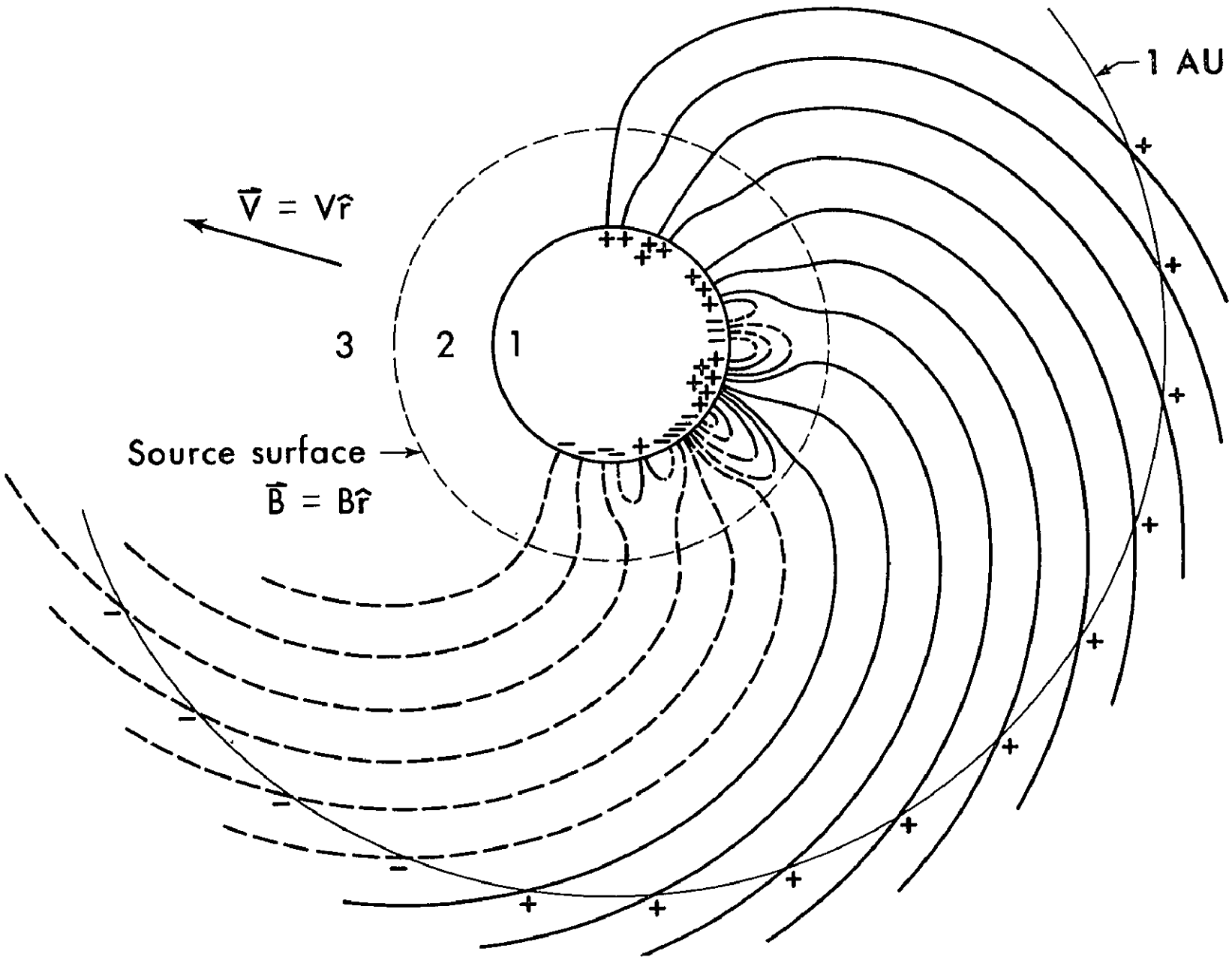

FIGURE 11

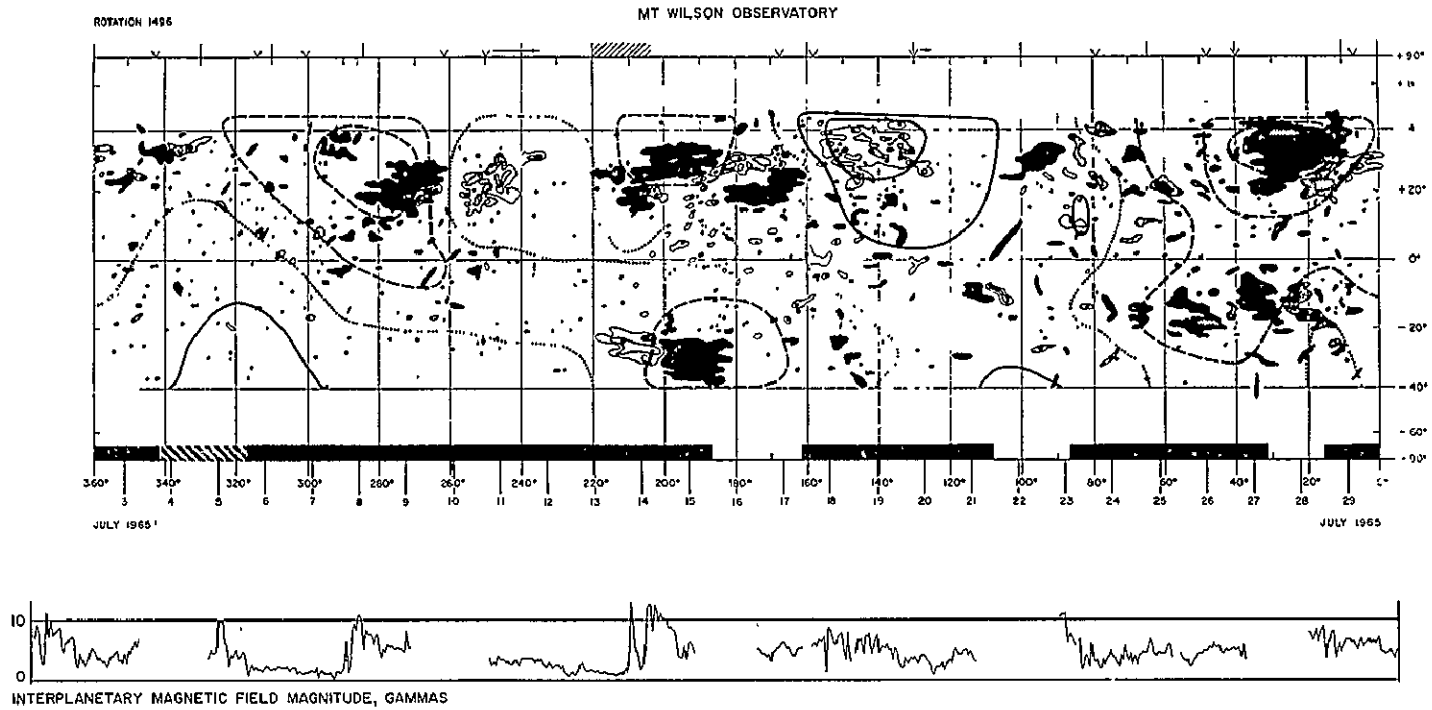
ROTATION 1496
MT WILSON OBSERVATORY
+90°
+40
+20°
0°
-20°
-40°
-60°
-90°
360°
340°
320°
300°
280°
260°
240°
220°
200°
180°
160°
140°
120°
100°
80°
60°
40°
20°
0°
3
4
5
6
7
8
9
10
11
12
13
14
15
16
17
18
19
20
21
22
23
24
25
26
27
28
29
JULY 1965
JULY 1965
10
0
INTERPLANETARY MAGNETIC FIELD MAGNITUDE, GAMMAS

FIGURE 12

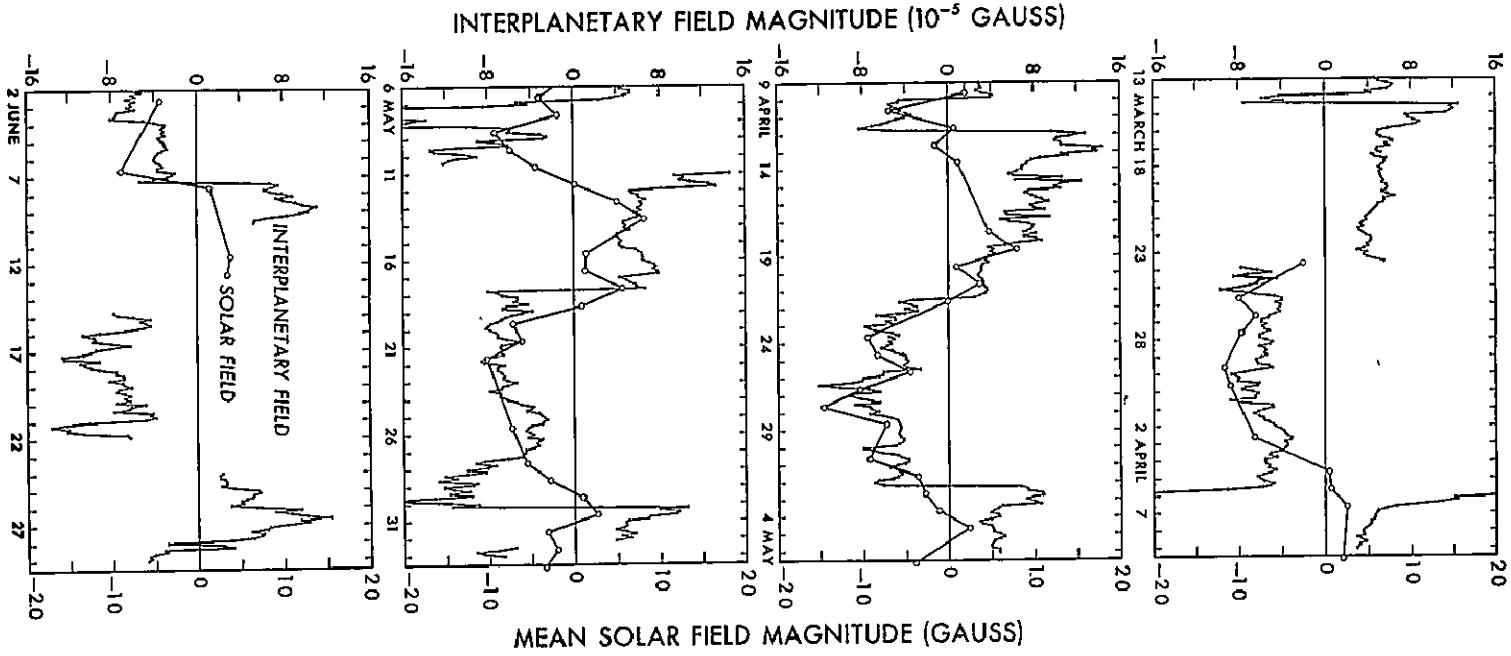
INTERPLANETARY FIELD MAGNITUDE (10^{-5} GAUSS)
MEAN SOLAR FIELD MAGNITUDE (GAUSS)
13 MARCH
18
23
28
2 APRIL
7
9 APRIL
14
19
24
29
4 MAY
6 MAY
11
16
21
26
31
2 JUNE
7
12
17
22
27
INTERPLANETARY FIELD
SOLAR FIELD

FIGURE 13

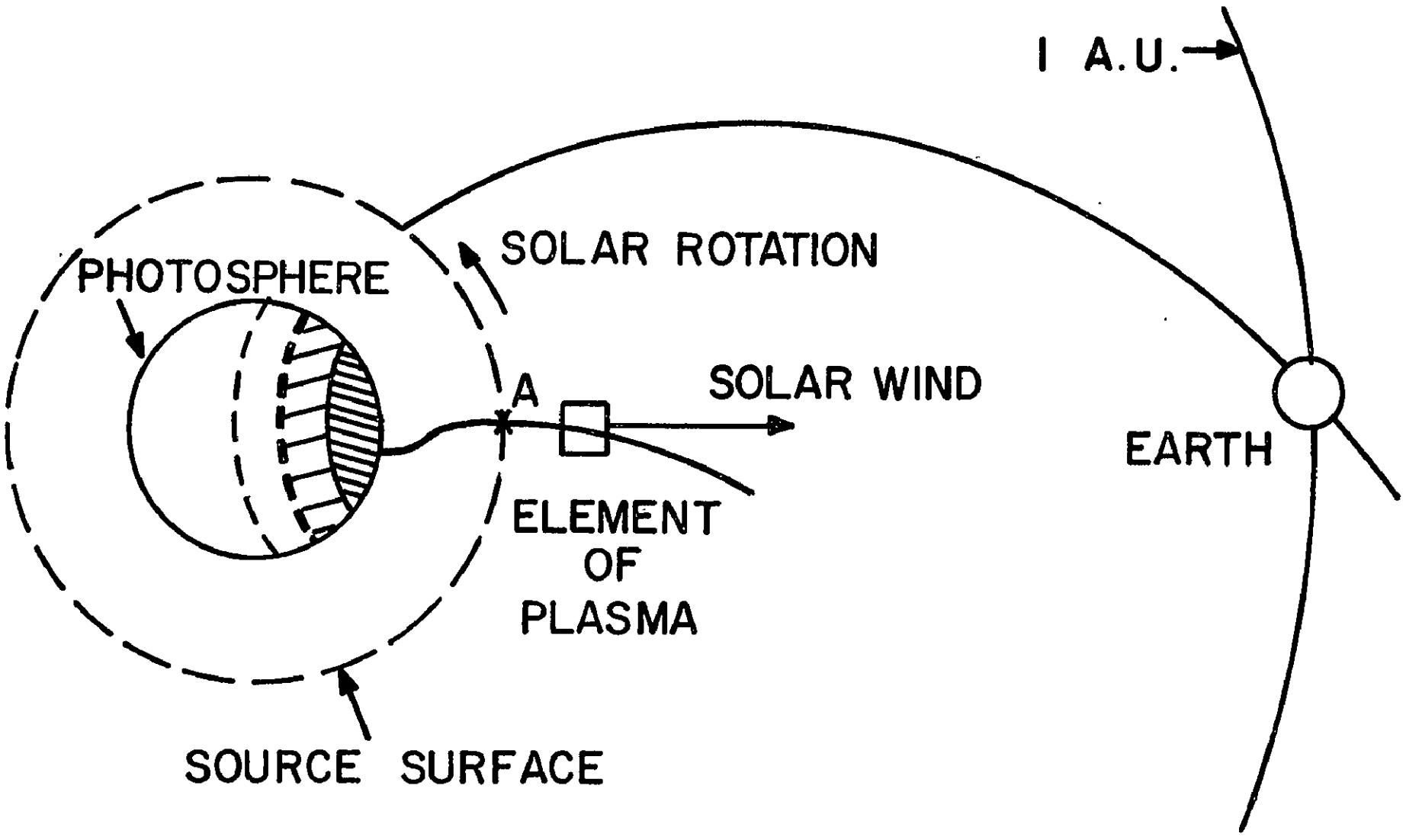
1 A.U.
SOLAR ROTATION
PHOTOSPHERE
A
SOLAR WIND
EARTH
ELEMENT
OF
PLASMA
SOURCE SURFACE

FIGURE 14

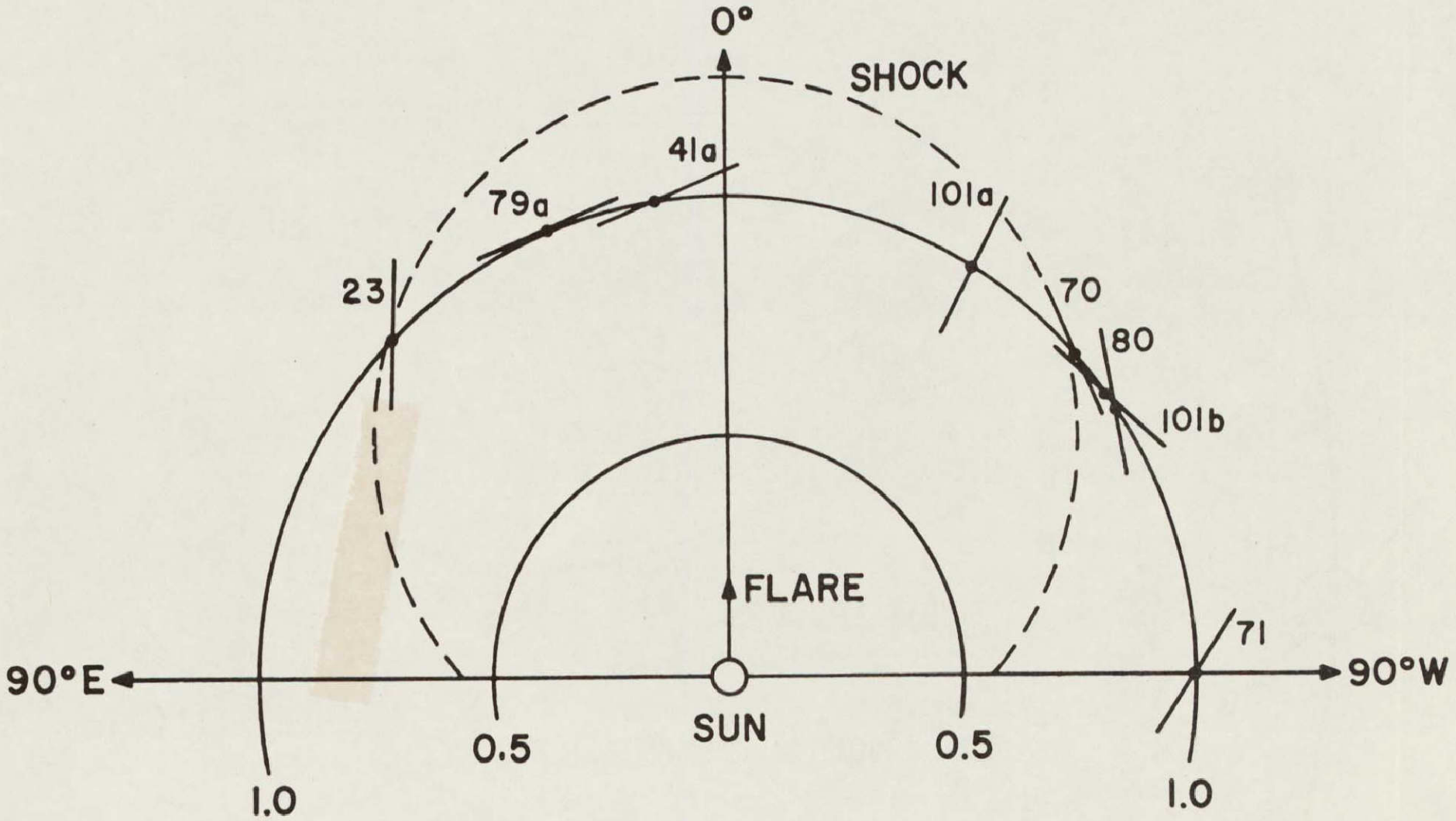
0°
SHOCK
41a
79a
101a
23
70
80
101b
FLARE
71
90°E
90°W
SUN
0.5
0.5
1.0
1.0

FIGURE 15

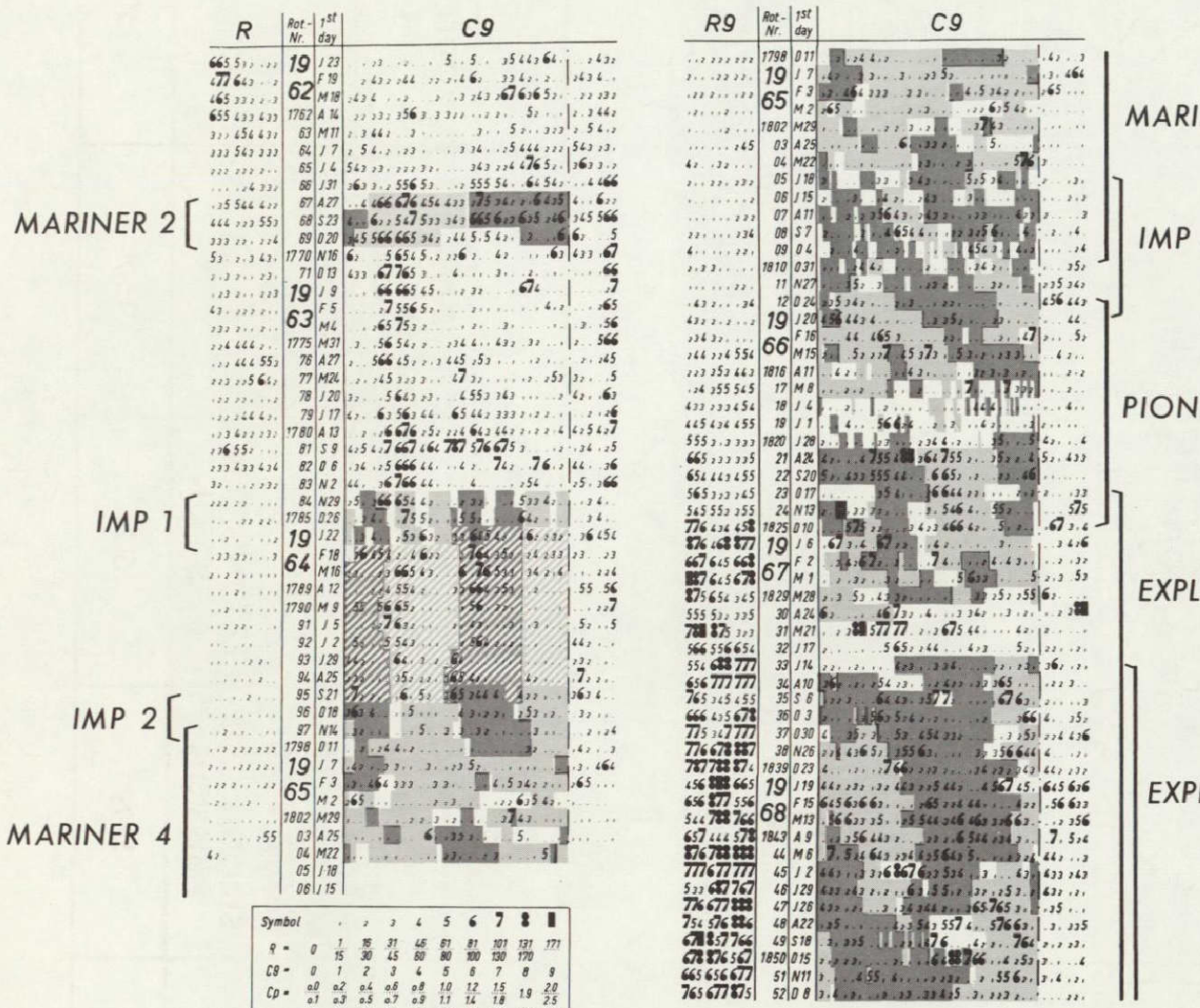

FIGURE 16

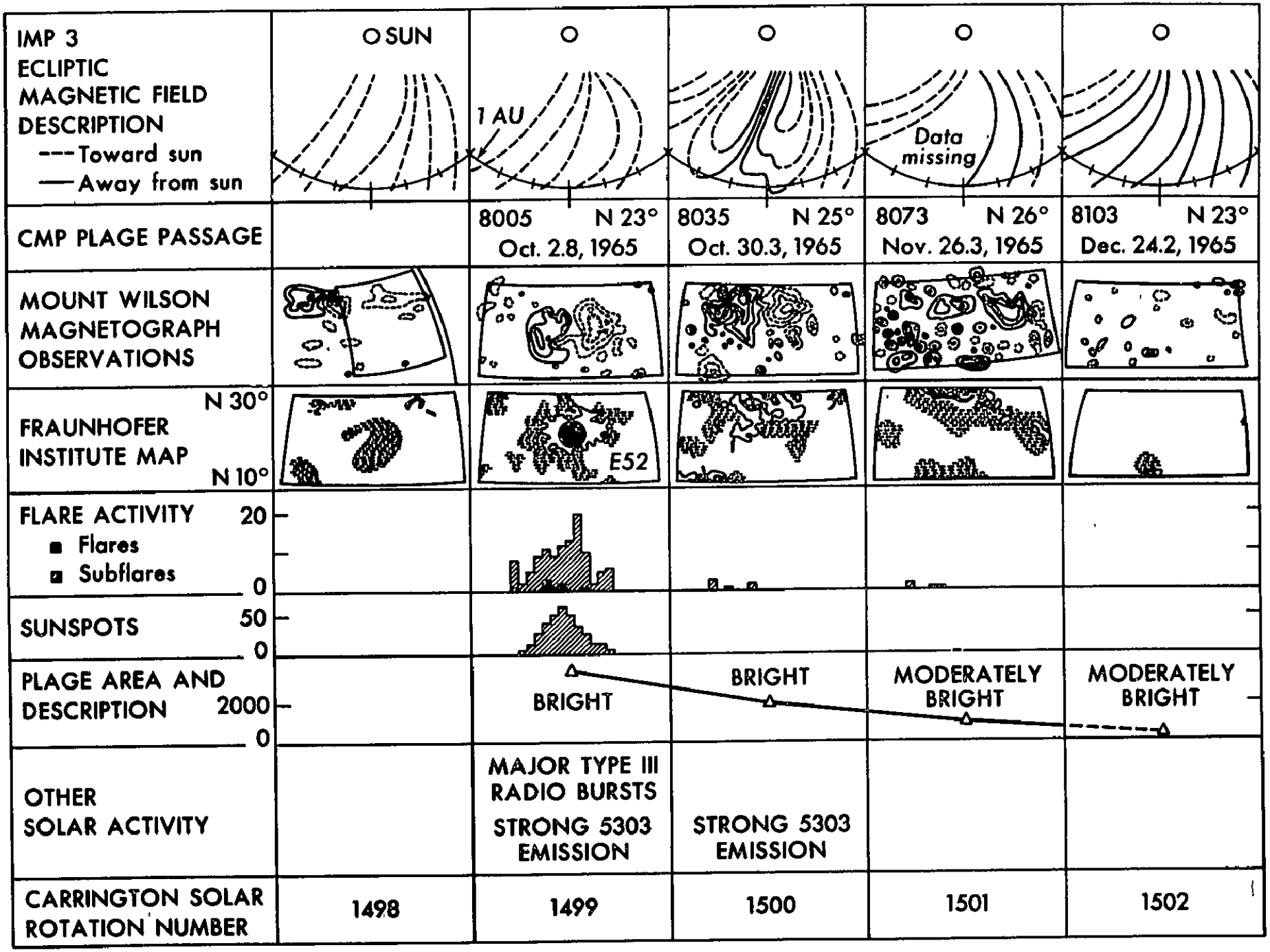
IMP 3
ECLIPTIC
MAGNETIC FIELD
DESCRIPTION
---Toward sun
—Away from sun
SUN
1 AU
Data missing
CMP PLAGE PASSAGE
8005 N 23°
Oct. 2.8, 1965
8035 N 25°
Oct. 30.3, 1965
8073 N 26°
Nov. 26.3, 1965
8103 N 23°
Dec. 24.2, 1965
MOUNT WILSON
MAGNETOGRAPH
OBSERVATIONS
N 30°
FRAUNHOFER
INSTITUTE MAP
N 10°
E52
FLARE ACTIVITY
20
Flares
Subflares
0
SUNSPOTS
50
0
PLAGE AREA AND
DESCRIPTION
2000
0
BRIGHT
BRIGHT
MODERATELY
BRIGHT
MODERATELY
BRIGHT
OTHER
SOLAR ACTIVITY
MAJOR TYPE III
RADIO BURSTS
STRONG 5303
EMISSION
STRONG 5303
EMISSION
CARRINGTON SOLAR
ROTATION NUMBER
1498
1499
1500
1501
1502

FIGURE 17

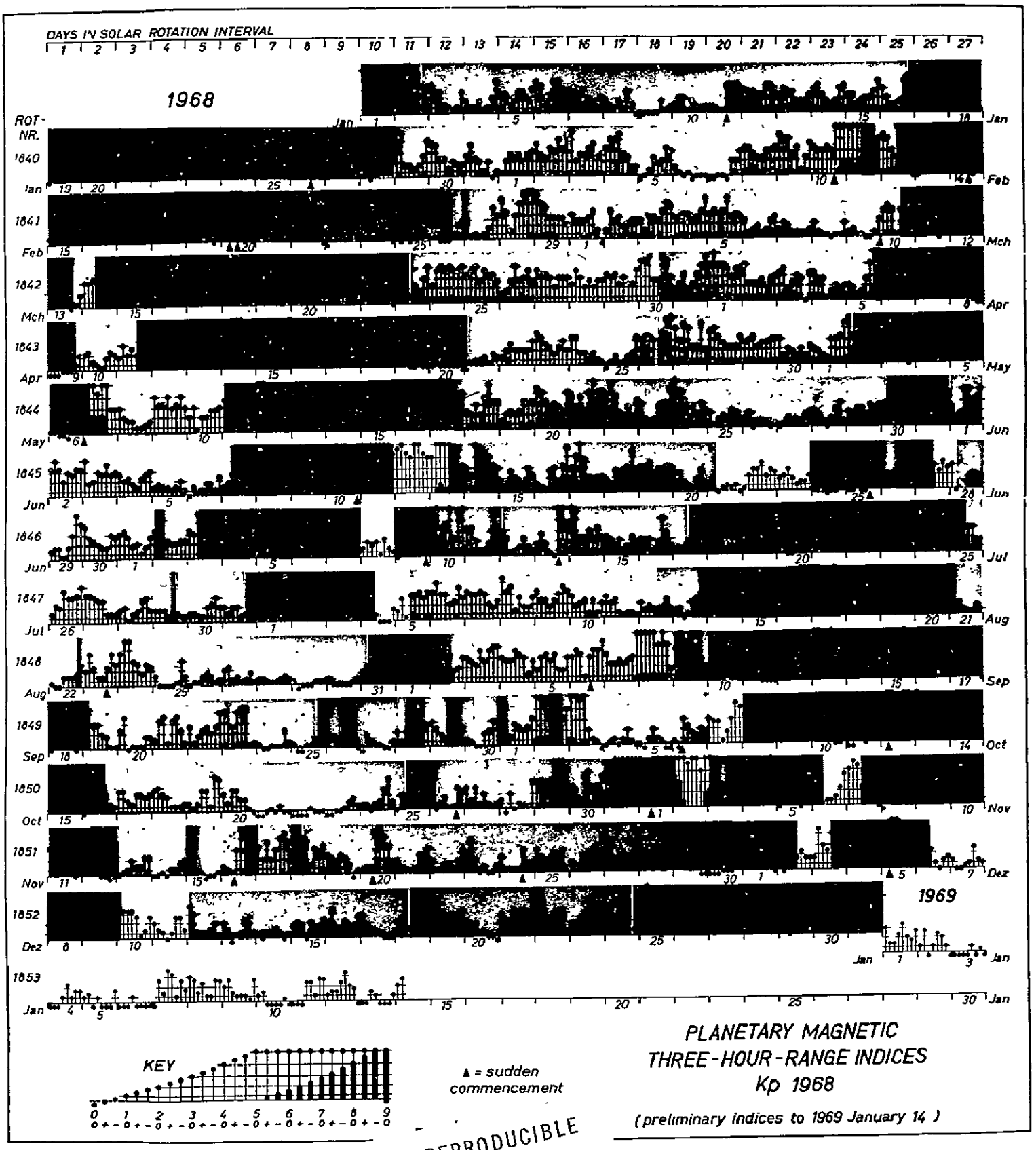

FIGURE 18

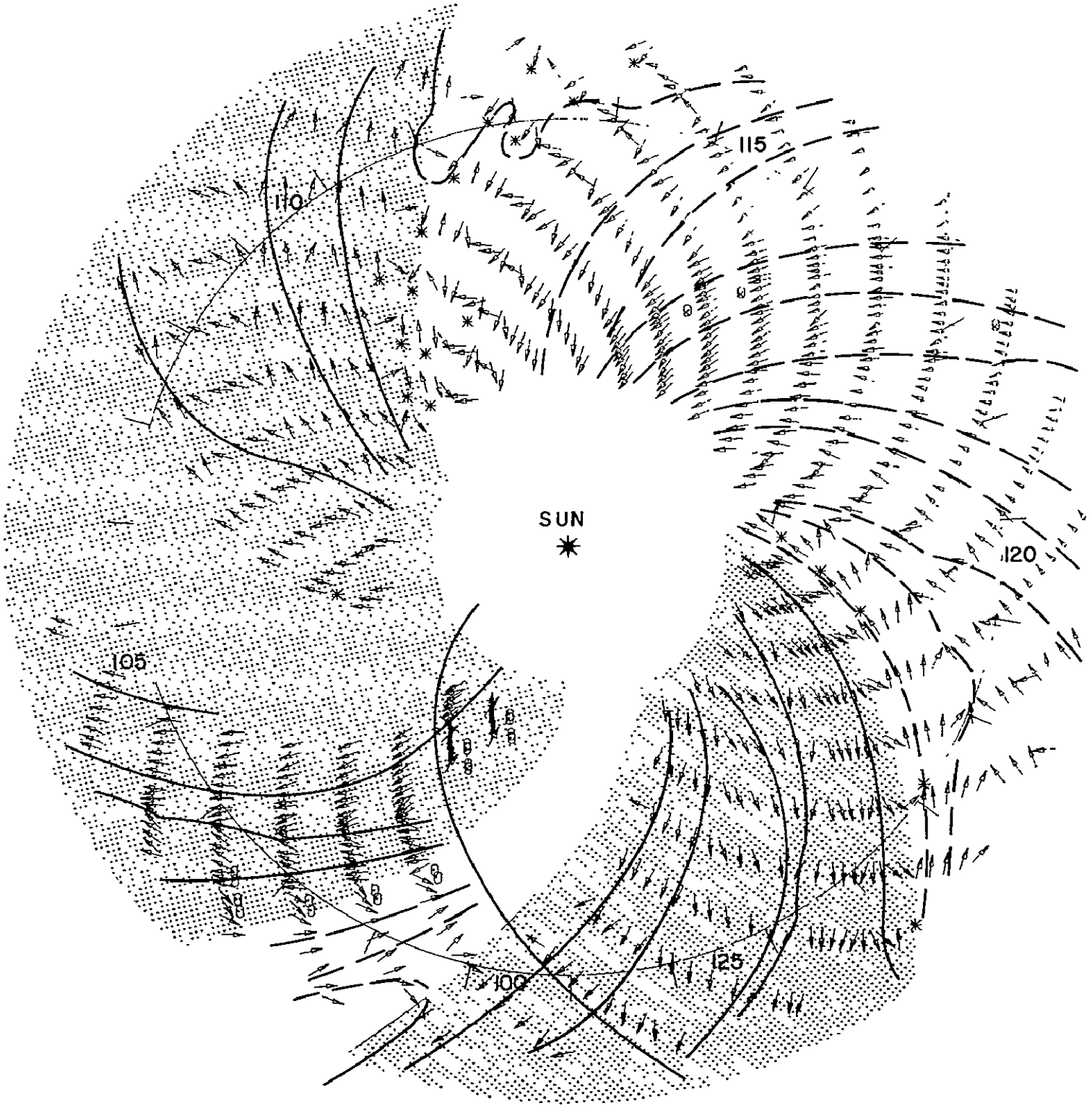

BARTELS' ROTATION 1843
APRIL 9, 1968 - MAY 5, 1968
100/68 - 126/68

FIGURE 19

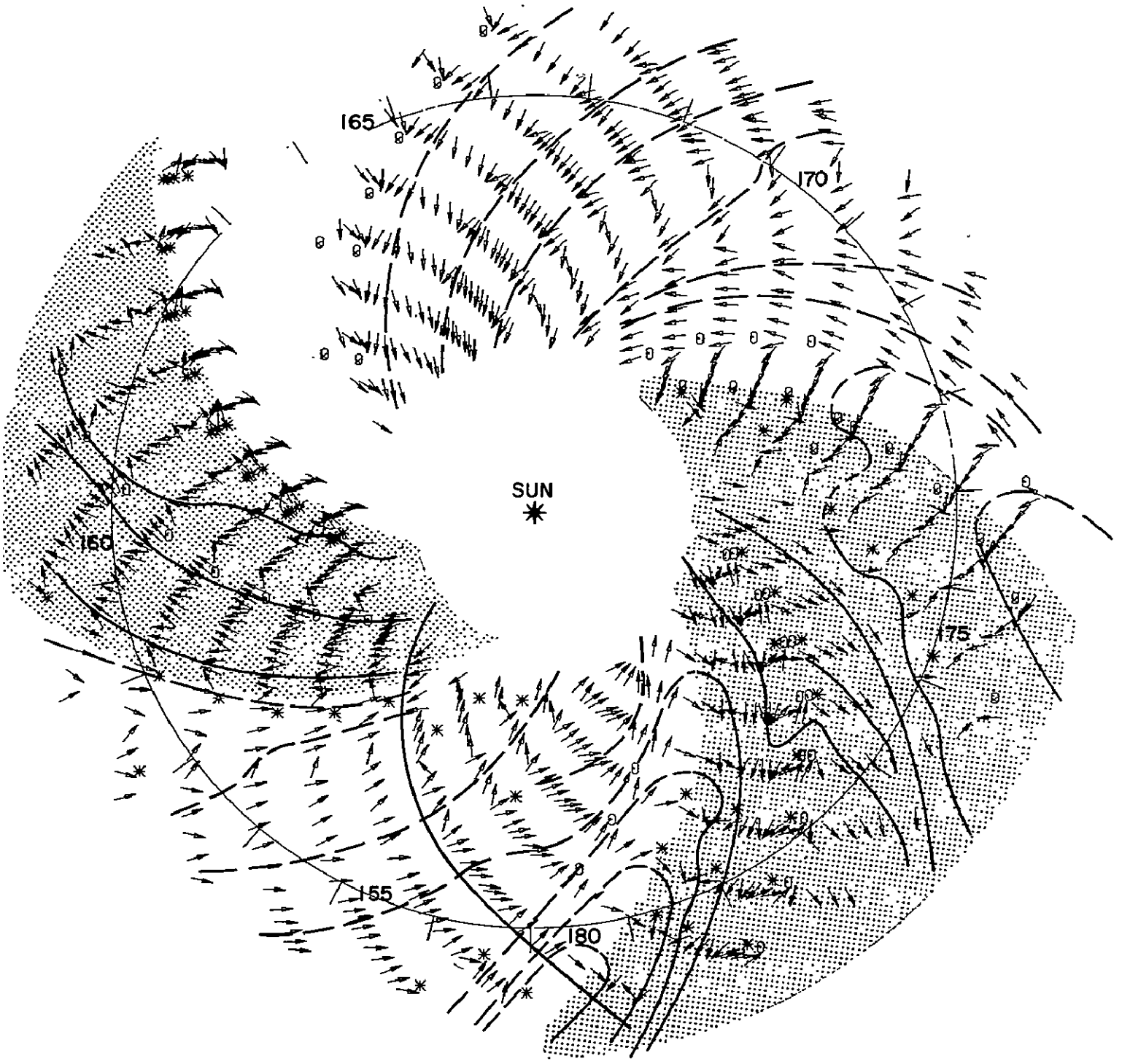

BARTELS' ROTATION 1845
JUNE 2, 1968 - JUNE 28, 1968
154/68-180/68

FIGURE 20

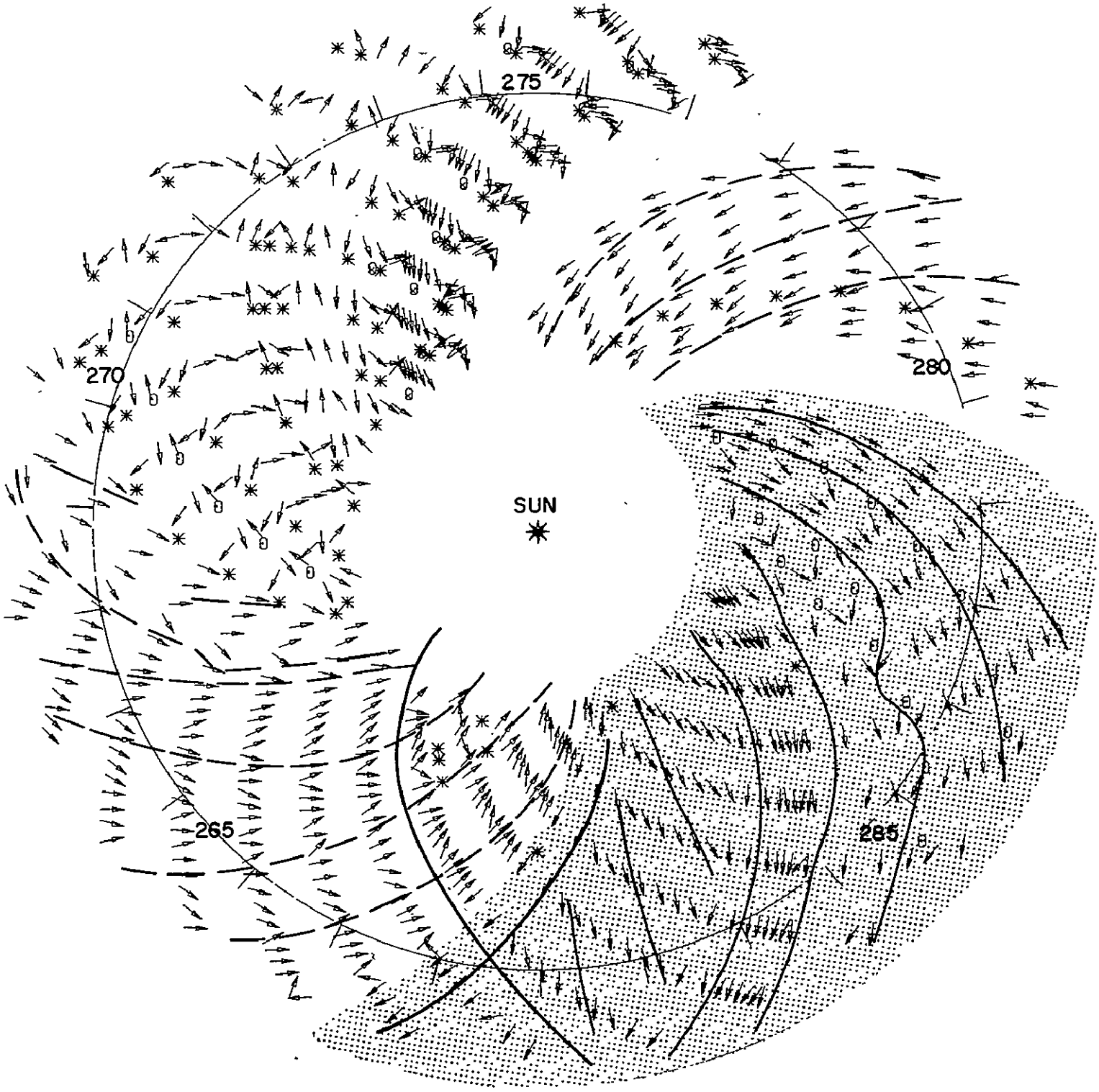

BARTELS' ROTATION 1849
SEPT 18, 1968-OCT 14, 1968
262/68 - 288/68

FIGURE 21

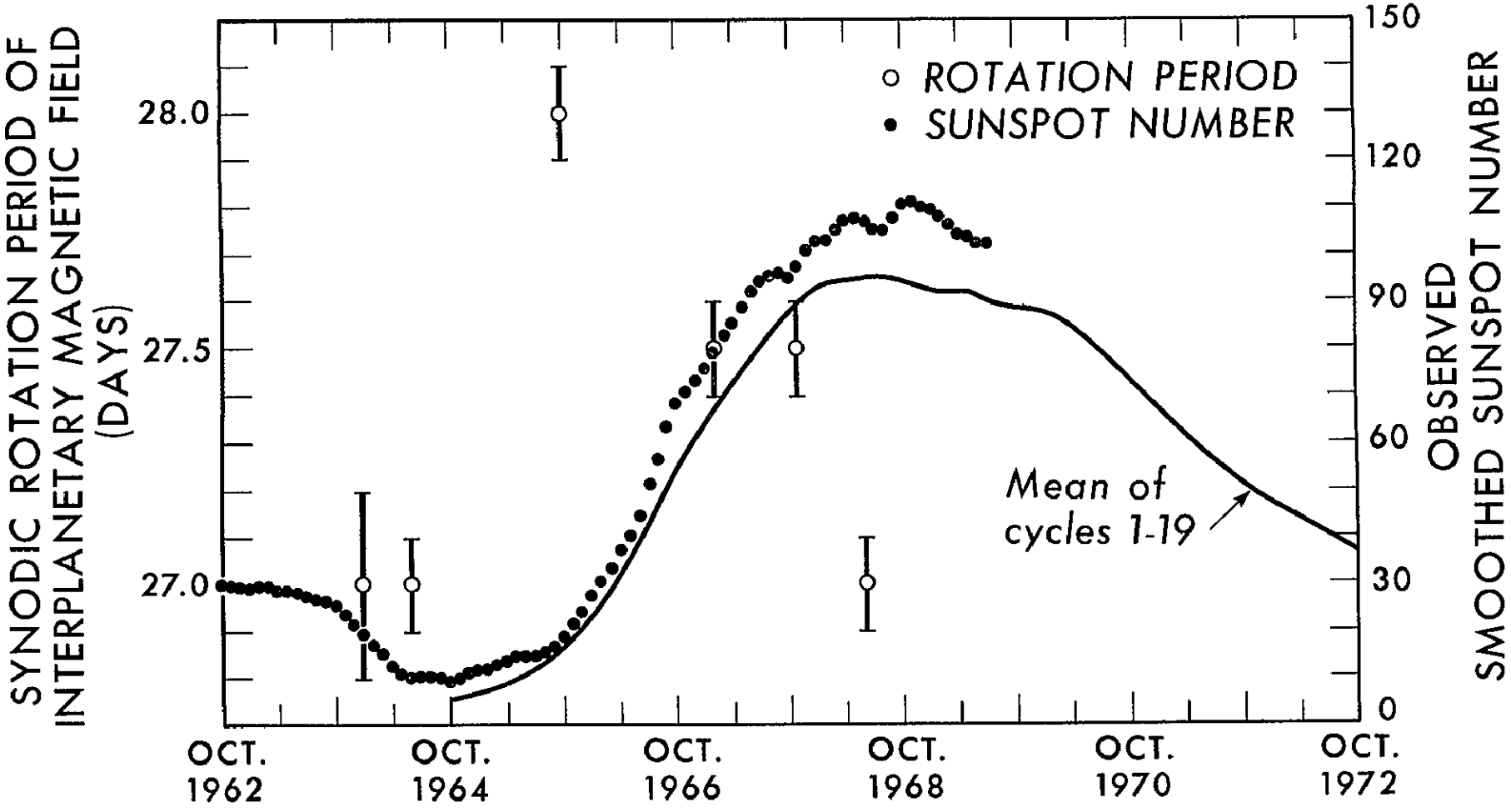
SYNODIC ROTATION PERIOD OF INTERPLANETARY MAGNETIC FIELD (DAYS)
28.0
27.5
27.0
ROTATION PERIOD
SUNSPOT NUMBER
Mean of cycles 1-19
150
120
90
60
30
0
OBSERVED SMOOTHED SUNSPOT NUMBER
OCT. 1962
OCT. 1964
OCT. 1966
OCT. 1968
OCT. 1970
OCT. 1972

FIGURE 22

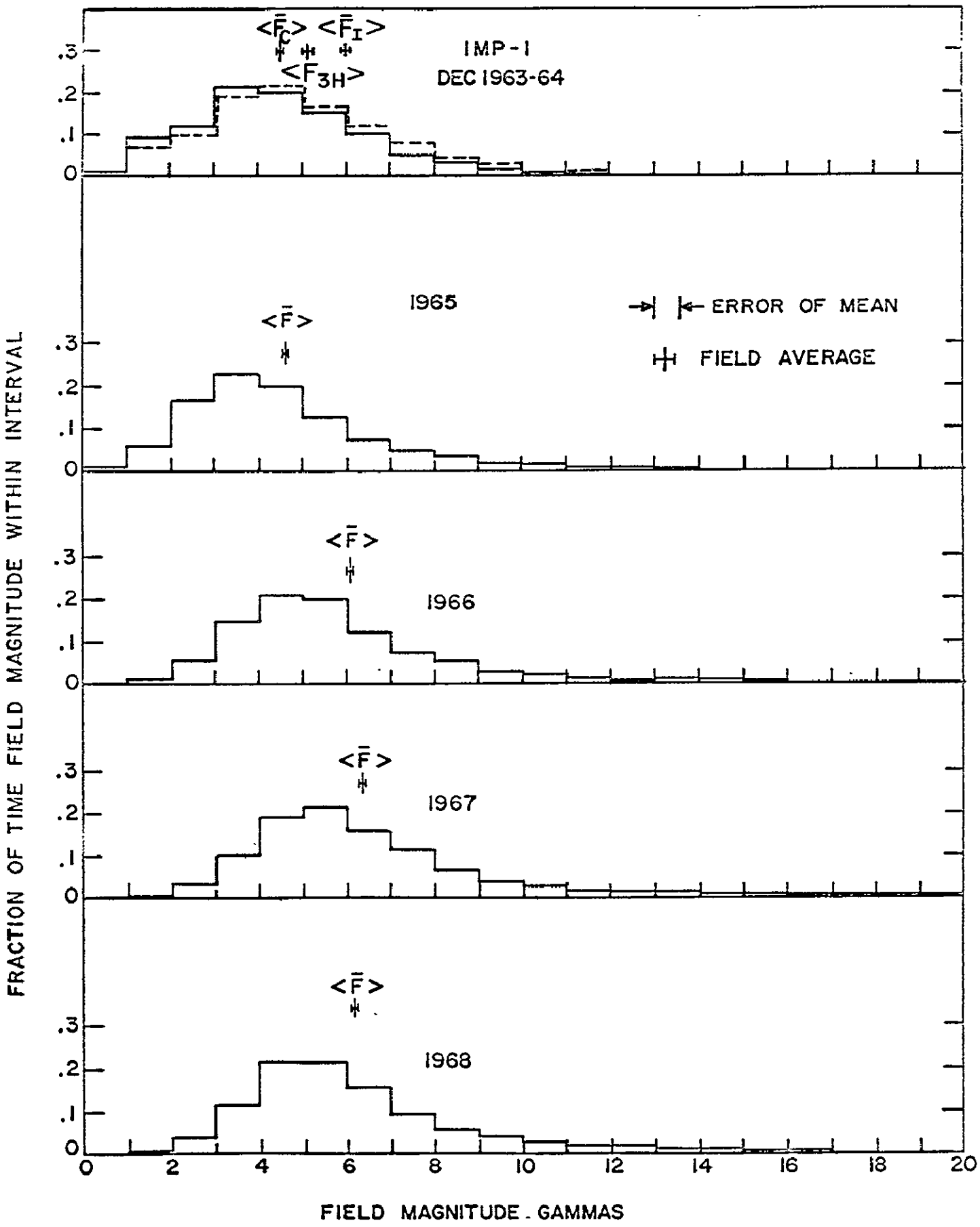
HISTOGRAM OF FIELD MAGNITUDE DISTRIBUTION
<F_C> <F_I>
<F_3H>
IMP-1
DEC 1963-64
1965
<F>
ERROR OF MEAN
FIELD AVERAGE
1966
1967
1968
FRACTION OF TIME FIELD MAGNITUDE WITHIN INTERVAL
FIELD MAGNITUDE - GAMMAS
0
.1
.2
.3
2
4
6
8
10
12
14
16
18
20

FIGURE 23

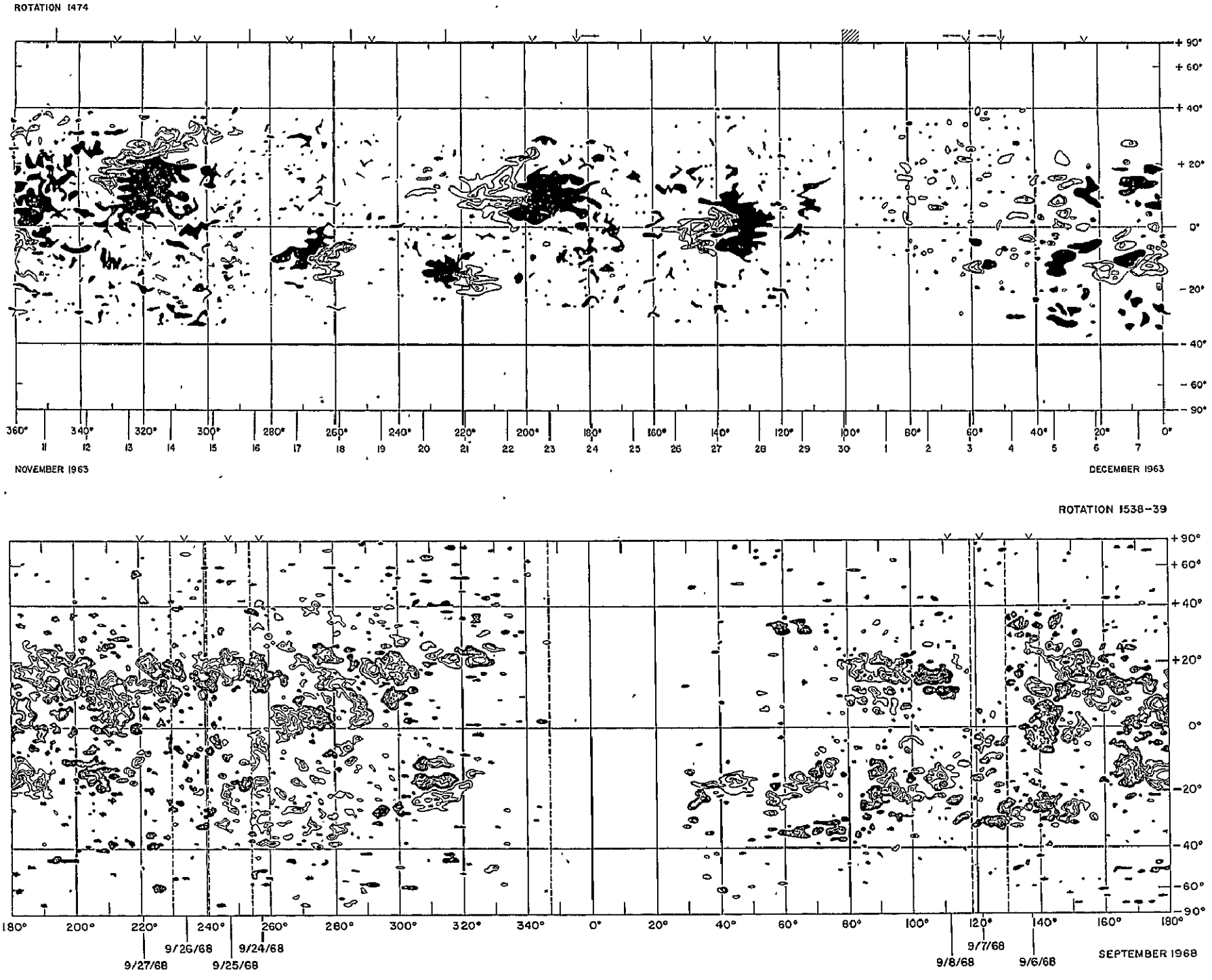
ROTATION 1474
+90°
+60°
+40°
+20°
0°
-20°
-40°
-60°
-90°
360° 340° 320° 300° 280° 260° 240° 220° 200° 180° 160° 140° 120° 100° 80° 60° 40° 20° 0°
11 12 13 14 15 16 17 18 19 20 21 22 23 24 25 26 27 28 29 30 1 2 3 4 5 6 7
NOVEMBER 1963
DECEMBER 1963
ROTATION 1538-39
+90°
+60°
+40°
+20°
0°
-20°
-40°
-60°
-90°
180° 200° 220° 240° 260° 280° 300° 320° 340° 0° 20° 40° 60° 80° 100° 120° 140° 160° 180°
9/27/68
9/26/68
9/25/68
9/24/68
9/8/68
9/7/68
9/6/68
SEPTEMBER 1968

FIGURE 24

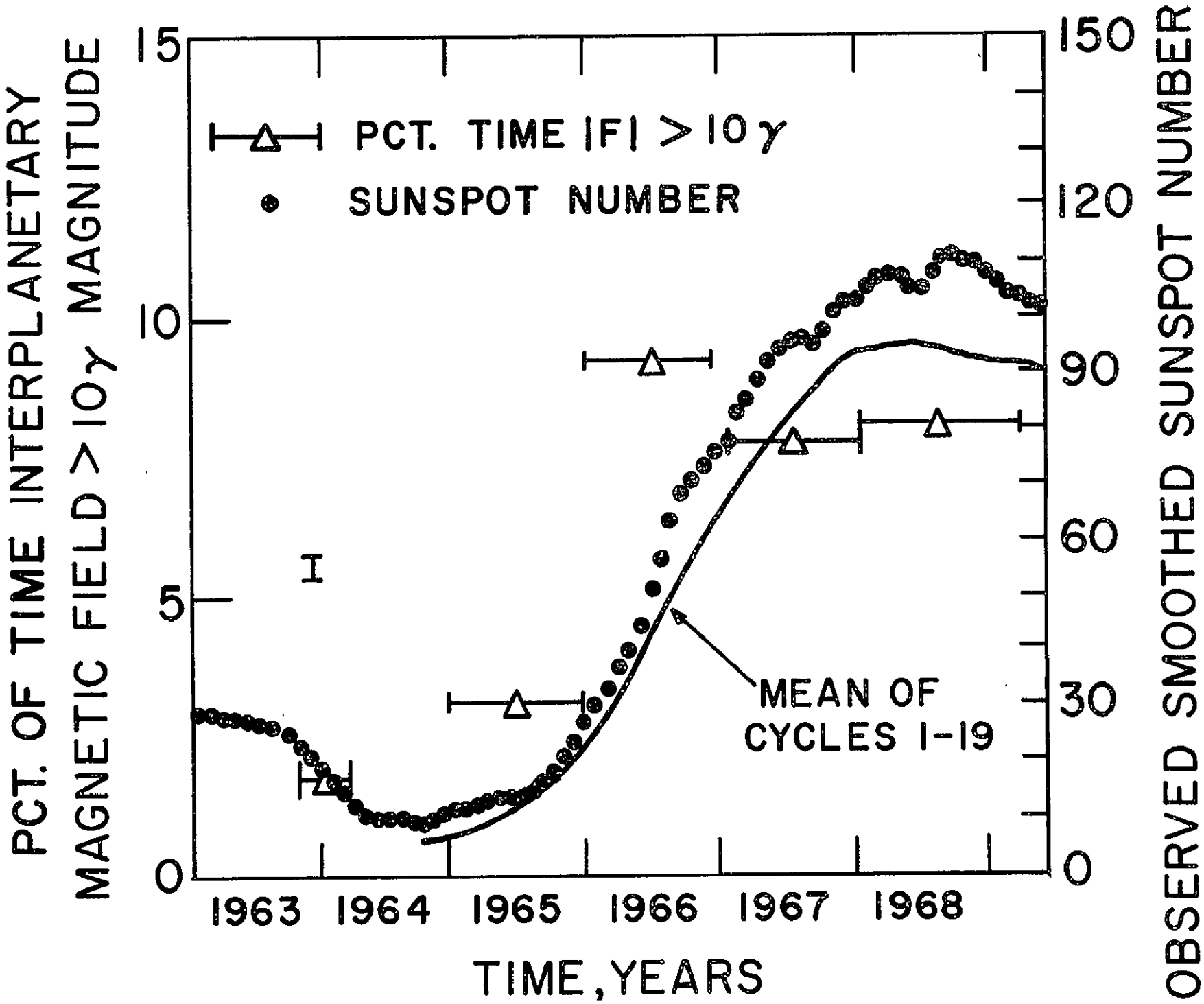
PCT. OF TIME INTERPLANETARY MAGNETIC FIELD > 10γ MAGNITUDE
OBSERVED SMOOTHED SUNSPOT NUMBER
PCT. TIME |F| > 10γ
SUNSPOT NUMBER
MEAN OF CYCLES 1-19
TIME, YEARS
0
5
10
15
30
60
90
120
150
1963
1964
1965
1966
1967
1968

FIGURE 25

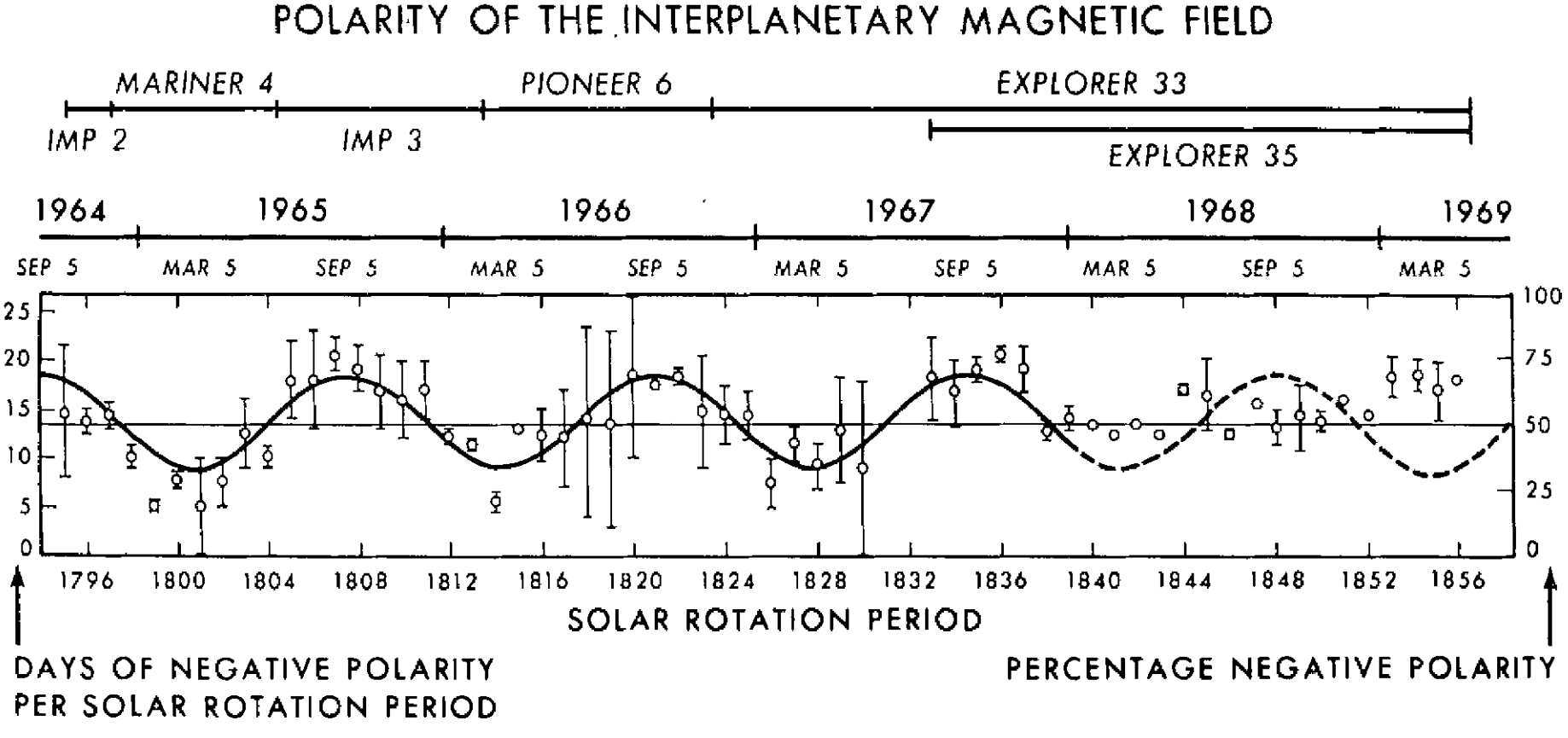
POLARITY OF THE INTERPLANETARY MAGNETIC FIELD
MARINER 4
PIONEER 6
EXPLORER 33
IMP 2
IMP 3
EXPLORER 35
1964
1965
1966
1967
1968
1969
SEP 5
MAR 5
SEP 5
MAR 5
SEP 5
MAR 5
SEP 5
MAR 5
SEP 5
MAR 5
25
20
15
10
5
0
100
75
50
25
0
1796
1800
1804
1808
1812
1816
1820
1824
1828
1832
1836
1840
1844
1848
1852
1856
SOLAR ROTATION PERIOD
DAYS OF NEGATIVE POLARITY
PER SOLAR ROTATION PERIOD
PERCENTAGE NEGATIVE POLARITY

FIGURE 26

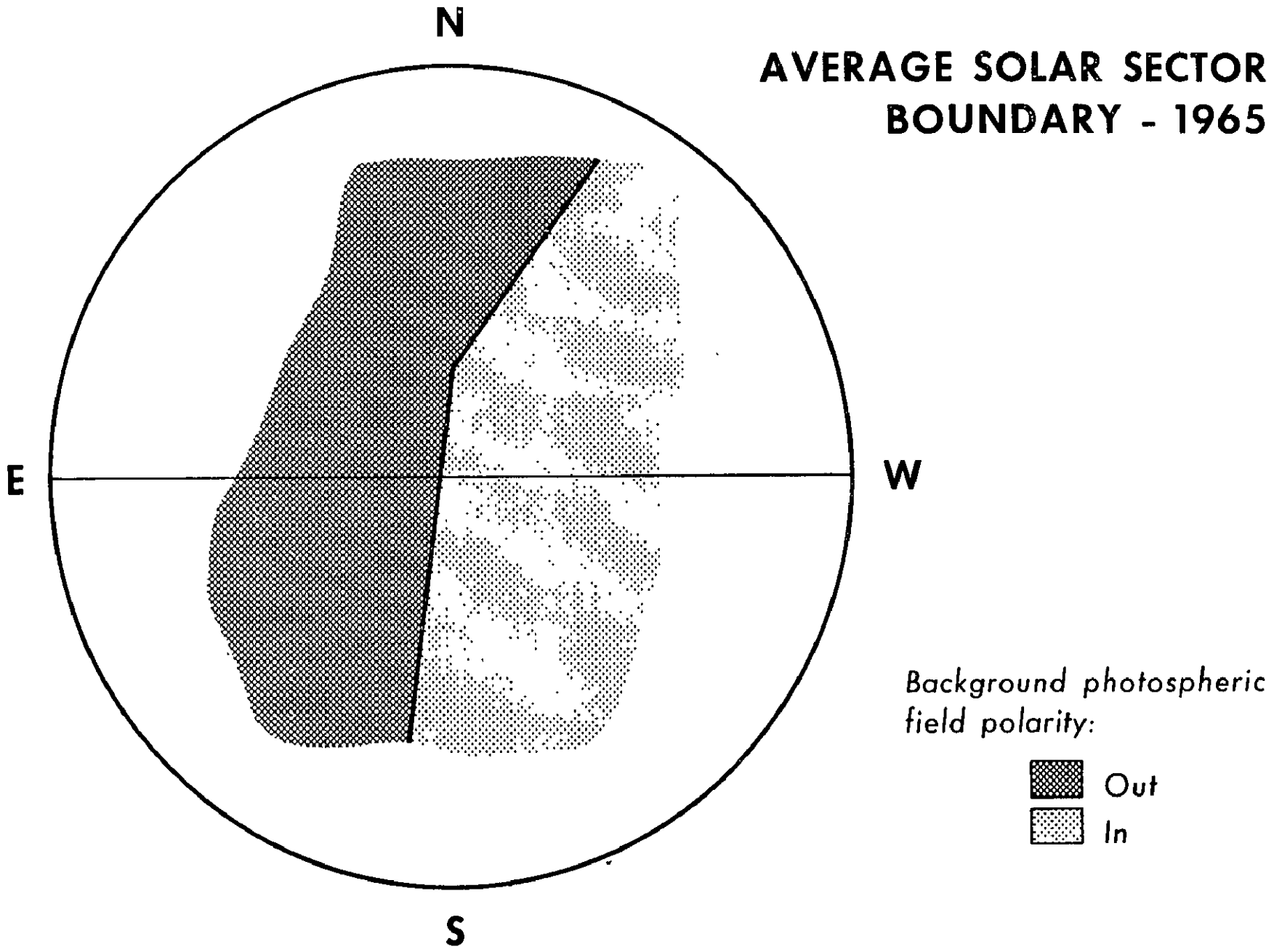
N
E
W
S
AVERAGE SOLAR SECTOR BOUNDARY - 1965
Background photospheric field polarity:
Out
In

FIGURE 27

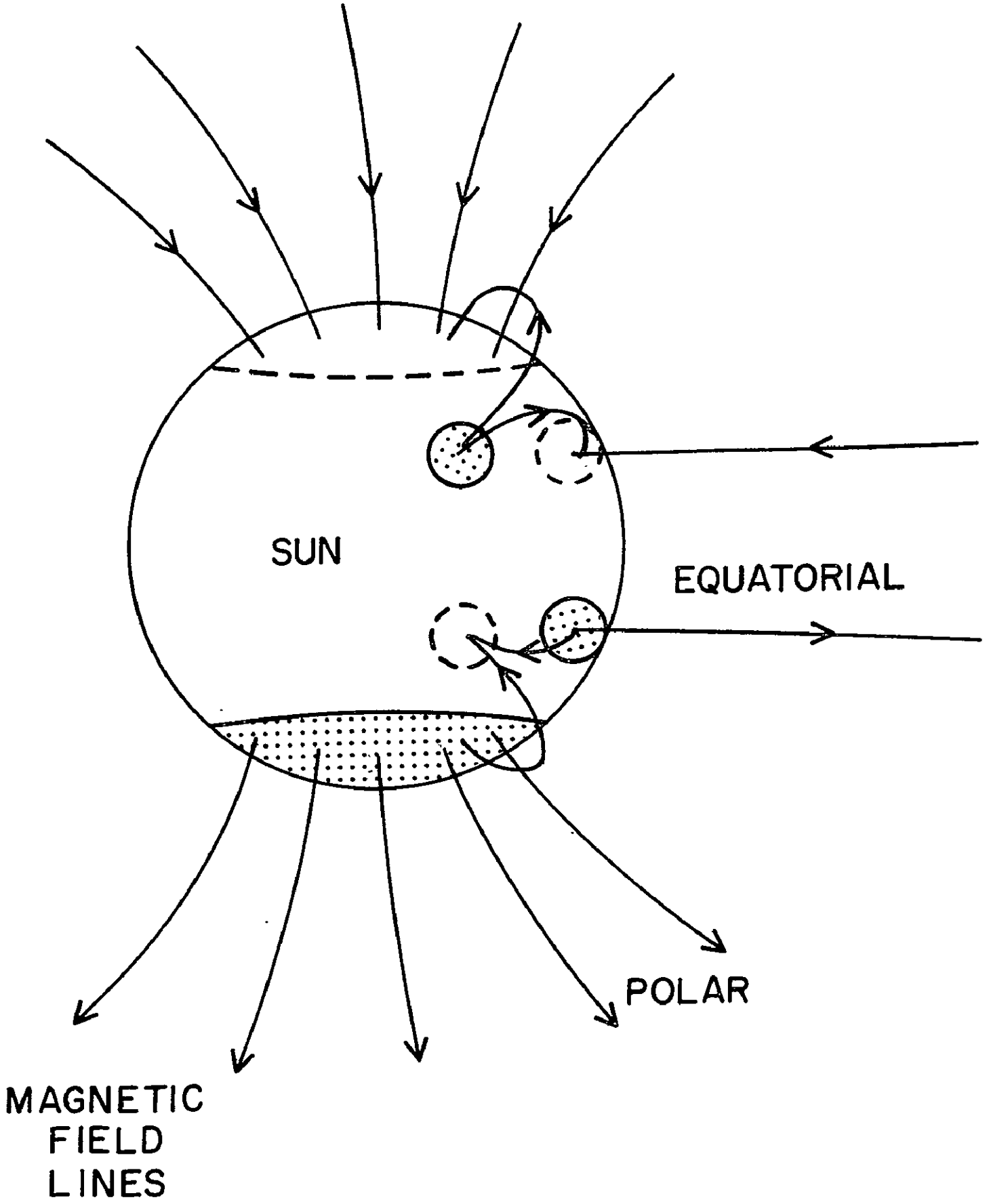

FIGURE 28

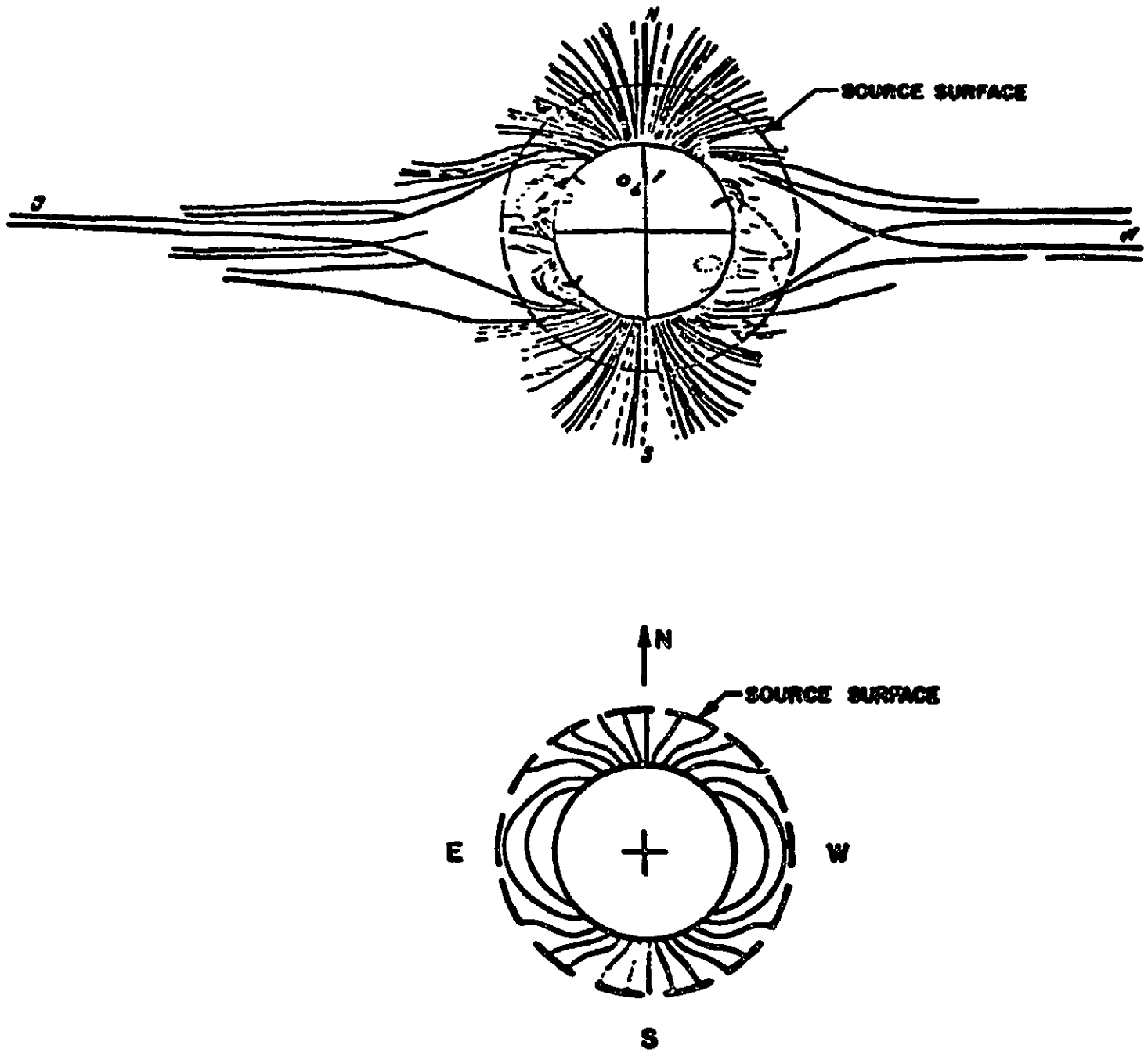

FIGURE 29

INTERPLANETARY FIELD STRUCTURES

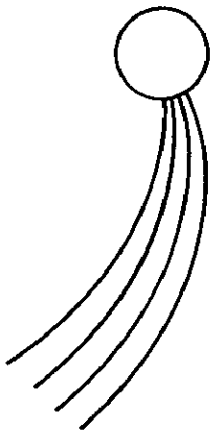

A] SPIRAL FIELDS

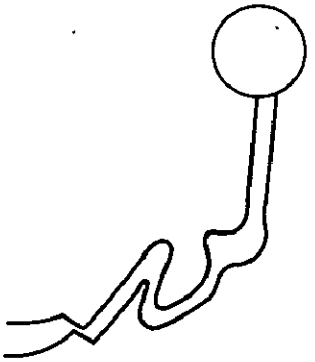

B] KINKS, WAVES OR VELOCITY PERTURBATIONS

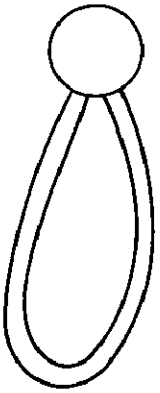

C] NEW FLUX LOOPS OF SOLAR ORIGIN

D] DECAYING SECTORS

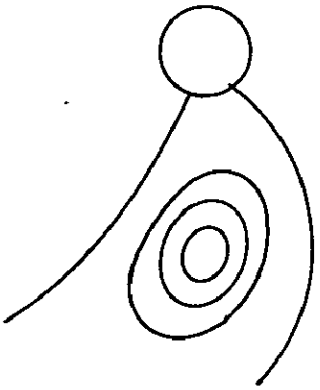

E] CLOSED MAGNETIC FIELD LOOPS

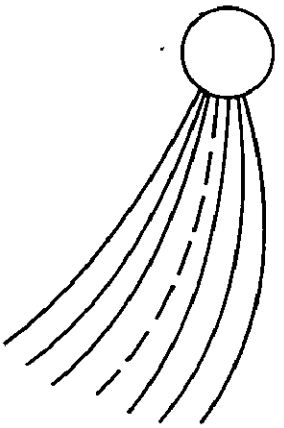

F] "FILAMENTS" OF SOLAR ORIGIN

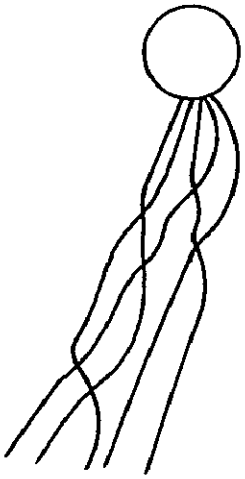

G] "BRAIDED" FIELDS

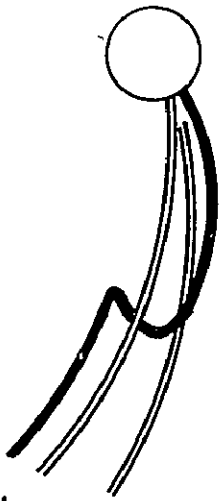

H] "SPAGHETTI" MODEL

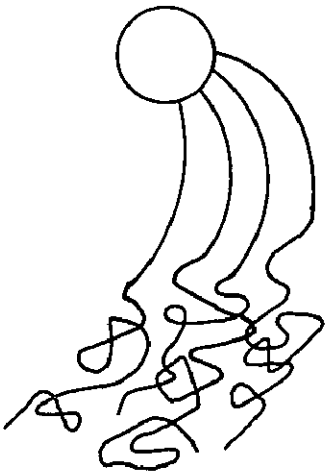

I] "CHAOTIC" FIELDS

FIGURE 30